Renewable and Sustainable Energy Reviews 21 (2013) 728–748

Contents lists available at SciVerse ScienceDirect

Renewable and Sustainable Energy Reviews

journal homepage: www.elsevier.com/locate/rser

An overview of combined absorption power and cooling cycles

Dereje S. Ayou [a], Joan Carles Bruno [a,*], Rajagopal Saravanan [b], Alberto Coronas [a]

[a] Universitat Rovira i Virgili, CREVER-Group of Applied Thermal Engineering, Avda. Paisos Catalans, 26, 43007 Tarragona, Spain
[b] Anna University, Institute for Energy Studies, Sardar Patel Road, Guindy, Chennai-600025, India

ARTICLE INFO

Article history:
Received 11 June 2012
Received in revised form
12 December 2012
Accepted 16 December 2012
Available online 28 February 2013

Keywords:
Combined power and cooling
Absorption cooling
Absorption power cycle
Waste heat
Solar energy

ABSTRACT

This paper presents an overview of the absorption cycles proposed in the literature for producing combined power and cooling. The dual output nature of these cycles makes it difficult to evaluate their performance so the various criteria used in the literature are presented and discussed. A combined system that simultaneously produces power and cooling can adapt to the whole range of energy demand – from only power to only cooling – with intermediate operation modes producing different ratios of power and cooling. This type of cycle uses highly concentrated ammonia vapour in the expander which can be expanded to a very low temperature without condensation and uses an absorption–condensation process instead of the conventional condensation process. The main advantage of these configurations is that they enable low-grade heat such as solar energy or waste heat to be used. The most suitable combined power and cooling systems for applications characterised by small-to-medium power and cooling capacities seem to be those that are directly derived from high-performance absorption chiller cycles.

Contents

1. Introduction

Energy-efficient and renewable energy technologies are being developed to reduce the high dependency of the European Union on energy imports, counter the rising prices of fossil fuels and fulfil the obligations for climate change protection. The commercial and residential building sectors are key actors in this strategy. In 2010 the services and residential sectors contributed 39.9% of the total final energy consumption in the European Union (EU-27), which was about 1153 Mtoe [1]. And in 2007 the services and residential sectors consumed 54.8% of the final electricity of the EU-27 member states [2]. Between 1999 and 2007 this EU-27 electricity consumption grew by 28.5% and 13.2% for the services and residential sectors, respectively [2]. One of the main applications of electricity is space heating and cooling. The consumption of electricity in the tertiary sector of the EU-27 (that is to say, the public sector, education, health care, services

* Corresponding author.
E-mail addresses: derejesendeku.ayou@urv.cat (D.S. Ayou), juancarlos.bruno@urv.cat (J.C. Bruno), rsaravanan@annauniv.edu (R. Saravanan), alberto.coronas@urv.cat (A. Coronas).

1364-0321/$ - see front matter © 2013 Elsevier Ltd. All rights reserved.
http://dx.doi.org/10.1016/j.rser.2012.12.068

Nomenclature

f	weight factor (dimensionless)
m	mass flow rate (kg/s)
η	efficiency
P	net power output (kW)
p	pressure (kPa)
Q	heat duty (kW)
t	temperature (°C)
T	temperature (K)
V	volume (m^3)
W	work (kJ)
X	ammonia mass fraction (kg ammonia/kg mixture)

Abbreviations

ACS	Advanced Cogeneration System
COP	Coefficient of performance (-)
EO	Equation-Oriented
EU	European Union
GRG	Generalized Reduced Gradient
GAX	Generator Absorber Heat Exchange
PC-SAFT	Perturbed Chain Statistical Associating Fluid Theory
RUE	Resource Utilization Efficiency
SF	Split Fraction
SPICE	Simulation Programme of Internal Combustion Engines
TR	Tons of Refrigeration
PSRK	Predictive Soave–Redlich–Kwong
SRK	Soave–Redlich–Kwong

Subscripts

A	absorber
B	boiler
C	condenser
E	evaporator
Ex	exergy
f	fan
G	generator
RB	reboiler
Rev	reversible
S	shaft
sg	steam generator

and commerce) for space and water heating and air conditioning is 22.6% of the total electricity consumed in the sector for the year 2007 [2].

Today, in the air-conditioning sector the dominant cooling systems are electrically driven compression chillers. To reduce the primary energy consumption of chillers, thermal cooling systems are an attractive alternative if solar energy or waste heat is used to produce cooling. If solar thermal energy is used for the air conditioning of buildings in summer, the seasonal cooling loads coincide with high solar radiation availability. In 2007, the number of solar cooling systems in Europe was estimated to be more than 250 with a cooling capacity of around 12 MW [3]. Because of its favourable climatic conditions Spain is one of the European countries in which the development of solar cooling is most attractive and it concentrates 27.5% of all the solar cooling installations in Europe, behind only Germany (39.1%) and in front of Greece (8.7%) [3]. The use of solar energy throughout the year for power, heating and cooling could increase the primary energy saving of a solar thermal installation and the economics of the investment.

In a conventional steam power cycle (Rankine cycle), the working fluid – usually water – is vaporized at high pressure and temperature and expanded through a turbine to produce mechanical or electrical power. Subsequently it is condensed and then pumped back to vaporize again in the boiler. The use of multi-component mixtures instead of pure fluids such as steam as the working fluid produces a better thermal match between the sensible heat source and the working fluid and there is less irreversibility during the heat-addition process, which increases the cycle efficiency. In the absorption power cycle, the working fluid only partially evaporates in the boiler and the remaining liquid can be used to absorb vapour in the absorber coming from the expander (turbine) outlet. This means, then, that the turbine back pressure is reduced not by the condensation process but by absorption–condensation.

The most commonly studied mixture for absorption power systems is ammonia–water. However, it should be pointed out that other multi-component mixtures can also be used [4–6]. Maloney and Robertson were among the first to study an ammonia–water based absorption power cycle [7] and found that it had no significant thermodynamic advantages over the steam-cycle configuration in the thermal boundary conditions considered. They did not consider the fact that ammonia–water mixtures can have lower temperature pinch points in counter current heat exchangers. The condensation process took place at a variable temperature and resulted in a higher turbine back pressure than that of the conventional steam Rankine cycle. This had a negative effect on power generation and cycle efficiency. In 1983 Kalina proposed an absorption power cycle [8] that had a slightly different configuration to the one studied by Maloney and Robertson. In this cycle (see Fig. 1) the vapour solution from the distillation unit (stream 5) is mixed with a bypass basic solution (stream 3). The combined stream (stream 6) is then cooled and condensed in a second condenser, which adds extra degrees of freedom to the system and allows the distillation unit to operate at a lower pressure than the boiler pressure. The lower pressure reduces the amount of energy required to separate the mixture, which improves the performance of the cycle. The mixture is heated, boiled, and superheated before it enters a turbine. Energy is recovered from the turbine exhaust and used to heat and partially boil the basic solution.

Similarly to the Rankine cycle which has several design options, Kalina cycle also has many special configurations, comprising a family of unique Kalina Cycle Systems (KCSs). Fig. 2 shows one of the simplest Kalina cycle configurations of the KCS family. It may be used with a combined heat and power plant (at the Industriepark Hoechst site in Frankfurt am Main, Germany) to improve the overall efficiency of the plant [9]. Each KCS in the family of designs has specific applications and is identified by a unique system number such as KCS5 (for direct fuel-fired plants), KCS6 (for gas turbine-based combined cycles, as a bottoming portion), KCS11 (for low-temperature geothermal plants), KCS34 (for low-to-medium temperature geothermal resources, as a topping thermodynamic cycle prior to district heating), etc [10–13]. The production of mechanical energy using absorption cycles of the Kalina type has a promising future and there are already a few manufacturers with a capacity range up to 6.5 MW and several countries have demonstration sites (Japan, Germany and Iceland) [9]. In 2011, Wasabi Energy announced that it had secured a contract with FLSmidth, through its subsidiaries, to build the largest Kalina cycle in the world [14]. This power plant will generate 8.6 MW of power from the waste heat available in the Khairpur cement plant (Pakistan).

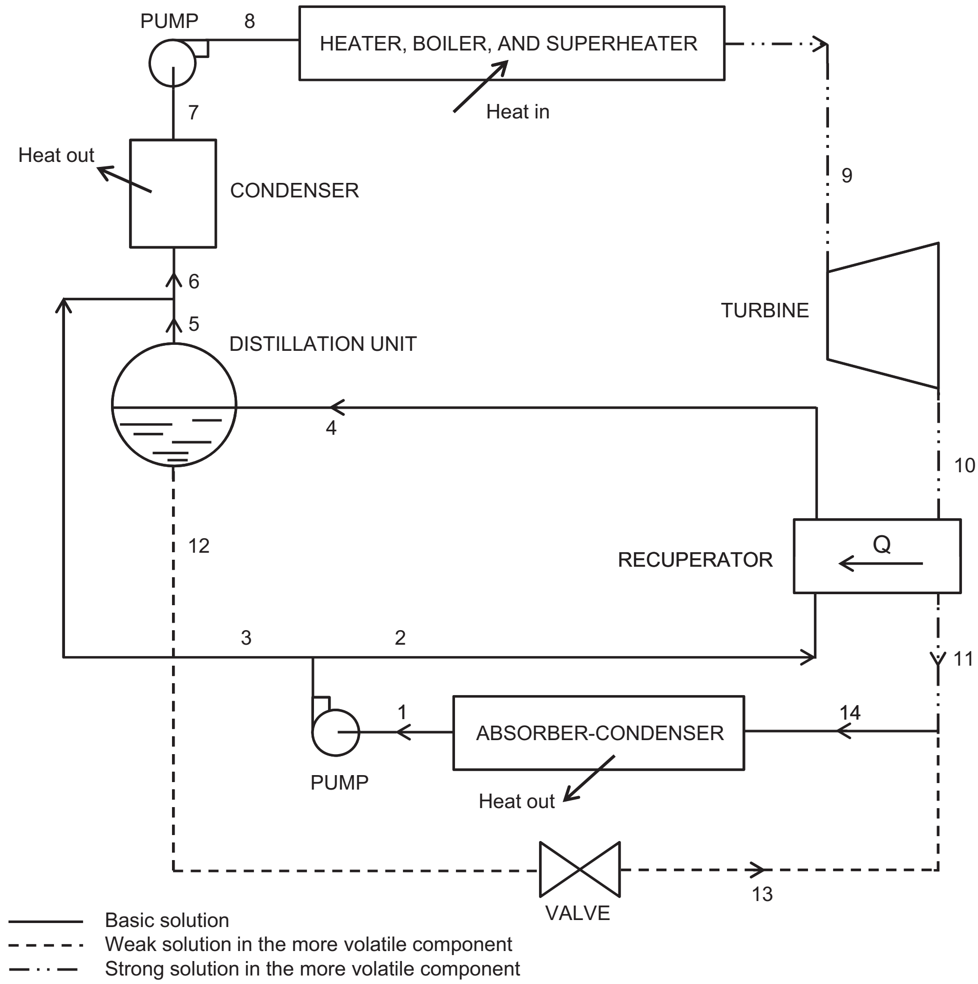


Fig. 1. Schematic diagram of Kalina power cycle proposed by Kalina [8].

The use of absorption chillers, however, is usually restricted to the summer season while in intermediate seasons they are only partially used. However, the power demand is almost constant throughout the year. A combined absorption system producing not only power as is the case for Kalina cycles but also cooling could be adapted to the whole range of energy demand, from only power to only cooling with intermediate operation modes that produce different ratios of each. The objective of this paper is to provide the technical details and current status of cycles proposed for combined power and cooling production suitable for applications such as buildings, which are characterized by small-to-medium power and cooling capacities. Building applications are also characterized by loads that change mainly due to ambient conditions. This paper does not deal with the combined production of power and cooling (refrigeration) from the waste heat generated by a thermal power plant to drive an absorption refrigeration system using heat integration; instead it focuses on the combined production of power and cooling (refrigeration) from the same thermodynamic cycle.

2. Fundamentals of absorption power and cooling systems

In this section the concept of absorption systems suitable for combined power and cooling applications is explained in terms of idealized energy conversion systems. They are described within the larger context of all the thermodynamic possibilities. An absorption cooling system can be regarded as a three-temperature-level, thermally driven chiller that uses heat (Q_2) at high temperature (T_2), produces cold (Q_0) at low temperature (T_0) and rejects heat (Q_1) to the atmosphere at medium temperature (T_1). Applying the first and second laws of thermodynamics for the system:

$$Q_2+Q_0-Q_1=0 \tag{1}$$

$$\frac{Q_2}{T_2}+\frac{Q_0}{T_0}-\frac{Q_1}{T_1}=0 \tag{2}$$

The chiller efficiency to describe the quality of the conversion of heat into cooling can be defined using the COP (Coefficient of Performance) that for a reversible absorption chiller is:

$$COP_{rev}=\frac{Q_0}{Q_2}=\frac{T_0}{(T_1-T_0)}\frac{(T_2-T_1)}{T_2} \tag{3}$$

The expression in Eq. (3) is frequently referred to as the Carnot COP for cooling production. The COP of an absorption chiller is lower than the Carnot COP (thermodynamic limit) since it accounts for both the internal and external irreversibilities.

The efficiency of a reversible thermal power plant can be defined as

$$\eta_{rev}=\frac{P}{Q_2}=\frac{T_2-T_1}{T_2} \tag{4}$$

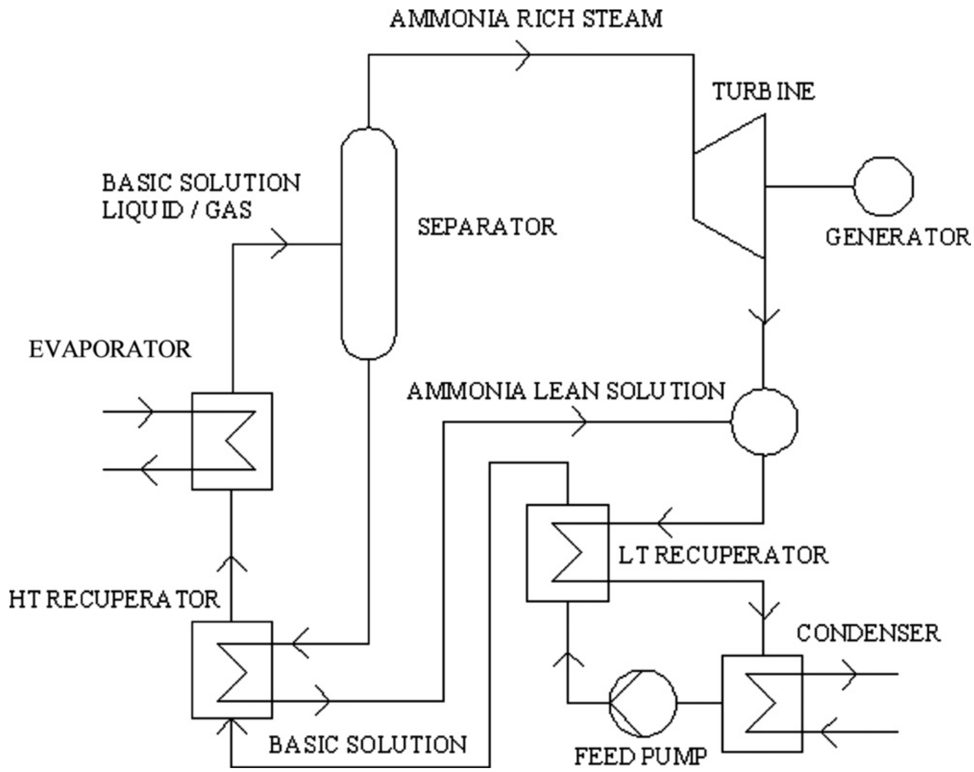


Fig. 2. Schematic of the simple Kalina power cycle configuration [9].

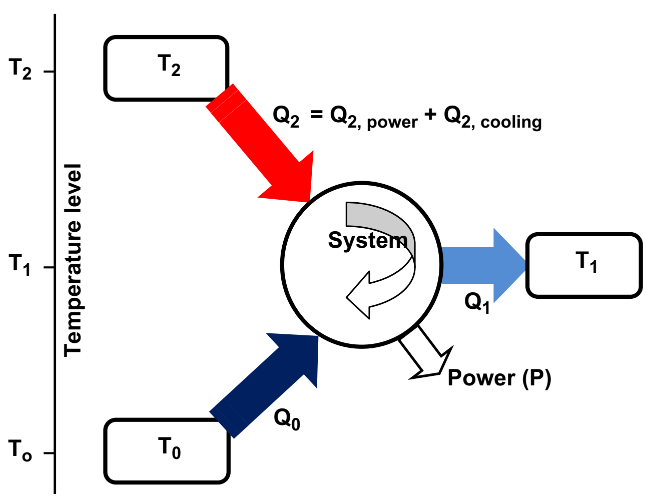


Fig. 3. A. diagram of absorption system for simultaneous generation of power and cold from a heat source.

$$COP_{rev} = \frac{T_0}{(T_1 - T_0)}\eta_{rev} \tag{5}$$

Comparing Eqs. (3) and (4) under similar thermal boundary conditions, it can be seen that the reversible power plant efficiency (Eq. (4)) has to be multiplied by the factor $T_0/(T_1-T_0)$, which is typically in the order of 10 [15]. This means that with similar low temperature heat sources significantly more cooling is produced (about ten times as much) than electrical energy.

2.1. Combined power and cooling

In a combined power and cooling system (see Fig. 3), the driving heat input (Q_2) is now the energy that is required to drive both the cooling and the power generation processes.

$$Q_2 = Q_{2,power} + Q_{2,cooling} \tag{6}$$

In this case, two independent parameters are needed to describe the performance of the system: the electrical efficiency (P/Q_2) and the cooling COP (Q_0/Q_2), or one of these plus the power-to-cold ratio (P/Q_0). Accordingly the following equations are obtained:

For reversible power and cooling processes:

$$\eta_{rev} = \frac{P}{Q_{2,power}} = \frac{T_2 - T_1}{T_2} \tag{7}$$

$$COP_{rev} = \frac{Q_0}{Q_{2,cooling}} = \frac{T_0}{(T_1 - T_0)}\frac{(T_2 - T_1)}{T_2} \tag{8}$$

By combining Eqs. (6) to (8), the following expressions for the performance parameters are obtained:

$$\frac{Q_0}{Q_2} = \frac{((T_2 - T_1)/T_2)(T_0/(T_1 - T_0))}{1 + (T_0/(T_1 - T_0))(P/Q_0)} = \frac{COP_{rev}}{1 + (T_0/(T_1 - T_0))(P/Q_0)} \tag{9}$$

$$\frac{P}{Q_2} = \frac{(T_2 - T_1)/T_2}{1 + ((T_1 - T_0)/T_0)(Q_0/P)} = \frac{\eta_{rev}}{1 + ((T_1 - T_0)/T_0)(Q_0/P)} \tag{10}$$

It can be seen that when power production is zero in Eq. (9) or the cooling is zero in Eq. (10) the problem reduces to the simple separate production of power and cooling.

There are two essential objectives when evaluating the performance of a cycle: one is to choose the parameters that lead to the best cycle performance; and the other is to compare the cycle with other energy conversion options [16]. Energy (first law), exergy and second law-based criteria are often used to assess the performance of energy conversion systems [17]. Since there are

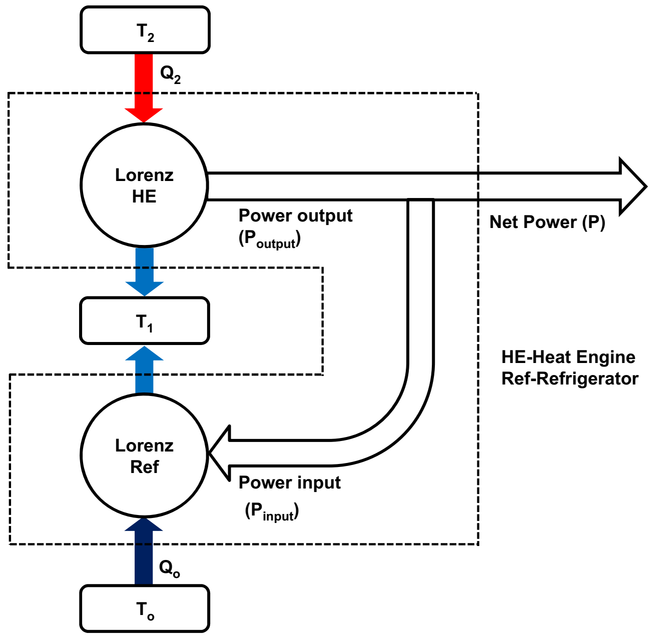


Fig. 4. Schematic diagram of cascaded Lorenz heat engine and refrigerator cycle.

two different kinds of simultaneous useful outputs (power and cooling), the quality of the cooling effect of the cycle needs to be determined in order to define its efficiency. To apply the conventional definition of second law efficiency for a combined power and cooling cycle, a suitable reversible cycle must first be defined.

For cycles with variable temperature heat addition and rejection processes, the corresponding reversible cycle is the Lorenz cycle [16]. For the same thermal boundary condition a cascaded Lorenz heat engine and refrigerator (Fig. 4) can define an ideal combined power and cooling cycle. The efficiency for a combined power and cooling cycle is as follows [16]:

When the cooling output of the cycle is weighted by a factor, f, to account for its quality:

- The energy (first law) efficiency (η_I):

$$\eta_I = \frac{(P + fQ_0)}{Q_2} \tag{11}$$

- Exergy efficiency (η_{ex}):

$$\eta_{ex} = \frac{(P + fQ_0)}{(E_{hs,in} - E_{hs,out})} \tag{12}$$

Since a sensible heat source provides the heat, the denominator in Eq. (12) is the change in exergy of the heat source.

In the literature, different weight factors (f) for the cooling produced by the combined power and cooling cycle are often used in the above efficiency expressions and in other similar efficiency expressions as well. The different cases are illustrated below:

Case I. In this case, the general form of the basic concept for measures of performance is defined as useful output per input for energy conversion systems. The energy (first law) efficiency of the combined power and cooling cycle is defined directly by adding the two different outputs (power and cooling) directly as useful output of the system. In this case, factor f in Eq. (11) is one ($f = 1$). In this type of first law efficiency definition, the quality of the cooling obtained from the combined cycle is not accounted for, results in the first law efficiency of the cycle being overestimated. In some cases it is closer to the thermodynamic limit of the first law efficiency or even exceeds it [16].

Case II. An appropriate and thermodynamically consistent way to account for the quality of the cooling, in first law and exergy efficiency definitions, produced by the combined cycle is to replace the cooling output of the cycle by the exergy associated with the cooling effect. This is equivalent to replacing the cooling output by the minimum work required to produce it, which means that the cooling output is weighted by the reciprocal of the reversible refrigeration cycle COP ($f = 1/COP_{rev}$). Efficiency expressions based on this weight factor can be used to compare the thermodynamically consistent performance of the combined cycle with other combined power and cooling producing options. However, in this case the cooling effect is not realistically weighted.

Case III. In order to weight the cooling output of a combined power and cooling cycle realistically, the cooling output must be weighted by a practically achievable cooling COP ($COP_{practical}$) or by dividing the exergy of the cooling by a reasonable second law efficiency for a refrigeration system. Therefore, the weight factor for this case is $f = 1/COP_{practical}$. On the basis of this factor the first law and exergy efficiencies of the combined power and cooling cycle are defined as follows. They are also referred to by Vijayaraghavan and Goswami as effective efficiencies [16].

$$\eta_{I,eff} = \frac{(P + Q_0/COP_{practical})}{Q_2} \tag{13}$$

$$\eta_{ex,eff} = \frac{(P + Q_0/COP_{practical})}{(E_{hs,in} - E_{hs,out})} \tag{14}$$

In some cases the combined power and cooling cycle operates in such a way that the output of the cycle is only power. Eqs. (13) and (14) can be used to compare the performance of a cycle that produces both power and one that produces only power.

For an identical cooling-to-power ratio (r) in the combined power and cooling cycle and the corresponding reversible cascaded cycle:

- Second law efficiency (η_{II}):

Using a weight factor f for the cooling, which is dependent on the thermal boundary conditions (Case II):

$$\eta_{II} = \frac{\eta_I}{\eta_{Lorenz}\left[1 + (r(f - 1/COP_{Lorenz})/1 + r/COP_{Lorenz})\right]} \tag{15}$$

The results of the idealised performance parameters presented in this section are independent of the working fluid properties. However, in real cycles the effect of the working fluid is of great importance and the method used to calculate its thermodynamic properties also has a significant effect (see section below).

3. Thermodynamic properties of ammonia–water mixtures

Many thermodynamic cycles have been used with such finite (sensible) sources as solar thermal, geothermal and waste heat to produce power using a pure component working fluid. In these cycles more than half of the driving heat transfer occurs during the boiling process. Since the boiler operates at essentially constant pressure, the temperature is also constant during the

boiling of the working fluid. This results in a mismatch between the temperature profile of the heat source and the working fluid. Consequently, there is significant exergy destruction during the process of heat addition in the boiler.

One of the methods that can be used to reduce this exergy destruction (or irreversibility) is to use multi-pressure boiling. The other option is to use non-azeotropic mixtures as a working fluid (e.g. ammonia–water) in a Kalina cycle. Non-azeotropic mixtures have variable boiling temperatures during a boiling process at constant pressure, which means that they provide a good thermal match with the sensible heat source [18].

Ammonia–water is the most extensively used binary mixture in absorption power cycles and combined power and cooling cycles. In power cycles, it has shown that it can provide higher thermal efficiencies than the conventional Rankine cycle with steam as a working fluid in different thermal boundary conditions [19–30]. The correlations for the thermodynamic properties of ammonia–water mixtures play a vital role in calculating the performance of the cycles. Most of the correlations that have been proposed [31–42] have been developed for pressures and temperatures that are lower than those commonly found in conventional power cycles. Table 1 shows the correlations that have been used in the literature to analyse ammonia–water absorption cycles with their pressure and temperature ranges. The theoretical bases of the correlations are also presented in Table 1.

To improve the cycle efficiency operating at high temperatures and pressures (nearly supercritical conditions), relevant data needs to be provided for regions beyond those covered by the present data. Absorption power and cooling systems that use the ammonia–water cycle can only be designed if accurate thermodynamic data of the mixtures is available over a wide range of T, p, X, including near and supercritical regions. Thorin et al. [44] compared the correlations developed by various sources [31–34]. The difference in saturation temperature for the different correlations is as high as 20%, and the difference in saturation enthalpy 100% when the pressure is 20 MPa.

Nowarski and Friend [45] presented an application of the one-fluid extended corresponding states method for calculating the thermodynamic surface of the ammonia–water mixture. The results show a strong temperature and composition dependence of both interaction parameters for the liquid, as well as for the vapour phase. Formulating the binary interaction parameters as functions of temperature and composition significantly improves the accuracy of density and pressure predictions. The authors also evaluated the statistical quality of the method using the data available on the thermophysical properties of the mixture.

The influence of various correlations for predicting thermophysical properties on determining the size of heat exchangers is reported by Thorin [46]. Different correlations for predicting the thermodynamic and transport properties give differences in the individual heat exchanger area of up to 24% and 10%, respectively. For the total heat exchanger area, the influence of the various correlations for the thermodynamic properties is 7% but for the transport properties it is not larger than 3%. A difference in the total heat exchanger area of 7% predicted by the thermodynamic properties would probably be less than 2% of the total cost of the process equipment.

Mejbri and Bellagi [47] formulated and compared three different approaches to model the thermodynamic properties of the ammonia–water refrigerant mixture. They are an empirical Gibbs free energy model, a semi-empirical approach based on the Patel–Teja cubic equation of state and a theoretical approach based on the PC-SAFT (perturbed chain statistical associating fluid theory) equation of state. The Gibbs free energy model is the most flexible and can describe the thermodynamic surface of the mixture up to 80 bar and 227 °C. It is used for medium temperatures and pressures, while the PC-SAFT equation of state is recommended for very high temperatures and pressures.

The PVTx properties of the ammonia–water mixture have been measured by Polikhronidi et al. [48] in the near and supercritical regions using a high-temperature, high-pressure, constant-volume adiabatic calorimeter–piezometer, along 40 liquid and vapour isochores between 120.03 and 727.75 kg/m^3, at temperatures between 28 and 36 °C and at pressures up to 28 MPa. Temperatures and densities at the liquid-gas phase transition curve, dew- and bubble-pressure points, and the critical parameters for the mixture were obtained using two different methods: namely, quasi-static thermograms and isochoric (P–T) break-point techniques. The derived and the measured values of the critical parameters such as temperature, pressure and density were found to be in close agreement.

The other ammonia–salt binary mixtures, such as ammonia–lithium nitrate (NH_3–$LiNO_3$) and ammonia–sodium thiocyanate (NH_3–NaSCN) can also be used in this type of system. The advantages they have over the conventional ammonia-water (NH_3–H_2O) are that the rectifier load and the generator temperatures are lower, which makes it possible to operate with simple flat-plate solar collectors. The information available

Table 1
Ammonia–water mixture property correlations range available in the literature.

Reference	Correlation basis	Application range	
		Pressure (bar)	Temperature (°C)
El-Sayed and Tribus [31]	EoS and Gibbs excess energy	0.1 to 110	27 to 499
Ibrahim and Klein [32]	Extension of Ziegler and Trepp model using measured data from [43]	0.2 to 110	−43 to 327
Park [33]	Based on the law of corresponding states	up to 200	up to 377
Stecco and Desideri [34]	EoS and Gibbs excess energy	up to 115	N.A
Smolen et al. [35]	Cubic EoS	up to 34	20 to 140
Moshfeghian et al. [36]	Cubic EoS and Group contribution theory	up to 35	up to 121
Ziegler and Trepp [37]	EoS and Gibbs excess energy	up to 50	up to 227
Ikegami et al. [38]	Benedict–Webb–Rubin EoS	up to 25	up to 107
Friend et al. [39]	Based on the law of corresponding states	up to 35	up to 177
Patek and Klomfar [40]	Empirical polynomial correlations	up to 20	up to 200
Tillner-Roth and Friend [41]	Complete thermodynamic model based on the Helmholtz free energy equilibrium equations	up to 400	N.A
Xu and Goswami [42]	Gibbs free energy method for mixture properties and empirical T_{bubble} and T_{dew} equations for vapour-liquid equilibrium	0.2 to 110	−43 to 327

EoS—Equations of State; T_{bubble}—Bubble point temperature; T_{dew}—Dew point temperature; N.A—Not Available.

on the thermophysical properties of these mixtures is limited [49–53].

4. Combined absorption power and cooling cycles

Combined power and cooling cycles use the waste heat rejected from the power cycle to run a coupled heat fired cooling cycle, such as an absorption refrigeration cycle, in which two cycles are combined to produce power and cooling [54,55]. As mentioned previously, such type of cycles are not covered in this review study. Moreover, cycles producing power and cooling (and/or heating) using the same thermodynamic cycle without involving absorption process are also beyond the scope of this study [56,57]. A unique feature of the combined power and cooling cycle proposed by Goswami [58,59] is that power and refrigeration (cooling) are simultaneously produced in the same loop. This cycle, also called the Goswami cycle, can be viewed as a combination of a NH_3–H_2O Rankine cycle and an absorption refrigeration cycle. In all of his studies Goswami used a binary mixture of ammonia and water, or some organic fluid mixtures, as the working fluid [6]. Other ammonia–water cycle configurations have been proposed by various researchers also for the production of power and cooling from the same cycle but using a different loop. This section focuses on the theoretical and experimental work of Prof. Goswami and others for generating power and cooling with the same cycle. The influence of the source of the ammonia–water mixture property database on the cycle performance parameters is also discussed.

4.1. Goswami cycle

The Goswami cycle (see Fig. 5) basically operates in the following way. A mixture of ammonia and water, known as a basic solution, is pumped from the absorber (state 1) to high pressure (state 2) via the solution pump. It is then split into two streams (state 2A and 2B) which, after recovering heat (state 13 and 14), mixes and enter the desorber (state 3) which is called a boiler by Goswami and co-workers. The mixture is partially boiled in the desorber to produce a vapour rich in ammonia (state 4) and a hot weak-in-ammonia liquid solution (state 10). A rectifier is used to increase the concentration of ammonia in the vapour, from the desorber, by partially condensing water out of it. The resulting purified vapour (state 6) is superheated (state 7) and expanded in the expander to produce power. Expanding the vapour (states 7–8) below the ambient temperature can simultaneously provide power and refrigeration. The refrigeration effect is obtained by sensible heating of the turbine exhaust (states 8–9). The weak liquid solution throttles back to the absorber after passing through a solution heat exchanger to recover heat from it (states 10–12). The vapour (state 9) and weak solution (state 12) are used to regenerate the basic solution in the absorber (state 1) and reject the heat from the cycle. In Fig. 5, the condensed liquid from the rectifier (state 5) is also mixed with the basic solution after recovering heat. Alternatively, it can be re-circulated into the desorber [60–62] or throttled back to be mixed with the weak solution [63].

The cycle can use waste heat, or solar thermal and geothermal energy, etc. as the source of heat. It can also work as a bottoming cycle for conventional power cycles. The cooling part of the cycle functions because the working fluid is a binary mixture (ammonia–water) and, at constant pressure, the condensing temperature of an ammonia-rich vapour can be significantly lower than the saturation temperature of a lower concentration ammonia–water mixture. To expand the vapour to low temperature in the expander requires a vapour with a high ammonia concentration and lower temperatures at the expander inlet, which does not favour power production. Obviously, superheating of the rectified vapour increases power production. But, it degrades cooling production. Since Goswami proposed the combined cycle a

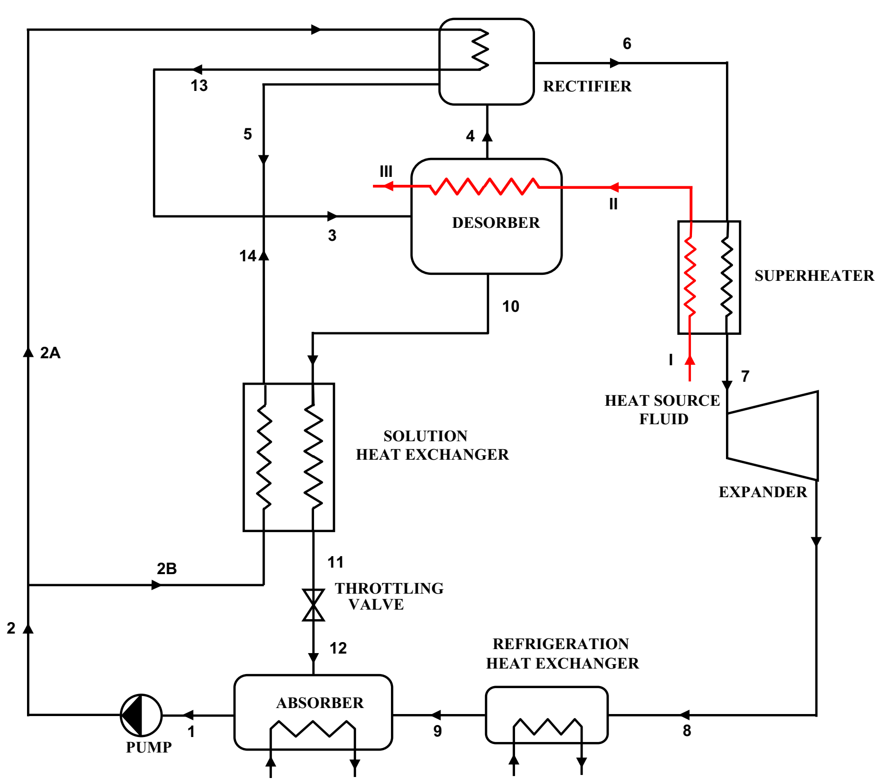


Fig. 5. Schematic diagram of the Goswami cycle with internally cooled rectifier.

number of studies have been made on such aspects as parametric analysis, optimisation of the cycle, refrigeration output at very low temperatures, and cycle modification for improving resource utilisation to mention just a few. These studies are reviewed below.

Goswami and Xu [60] conducted a parametric analysis to study the effect of the cycle parameters on the performance of the cycle. Application of low heat-source temperatures below 200 °C is one of the characteristics of this cycle. Since it uses the turbine exhaust gases by means of a cooler that transfers sensible heat from the chiller water, the cooling output is relatively small. They also reported a procedure for optimising the operating conditions of the cycle for thermal performance [61]. Under optimum conditions for a heat source temperature of 87 °C, both power and refrigeration outputs were achieved. At a source temperature of 167 °C, optimum conditions do not provide any refrigeration output. However, under non-optimum operating conditions a refrigeration output was also possible for the same source temperature.

Lu and Goswami [62] focused on the refrigeration part of the total output of the Goswami cycle at low refrigeration temperatures. The performance of the combined cycle was determined at a wide range of low refrigeration temperatures and for a heat source temperature of 87 °C. At each refrigeration temperature, the cycle was optimised for maximum second law efficiency using the Generalized Reduced Gradient (GRG) algorithm. The authors defined the second law efficiency as the ratio of the useful energy output from the cycle to the exergy consumption of the cycle. Based on the type of weight factor used for the refrigeration output, two different second law efficiency definitions were used in the optimisation process. Lu and Goswami gave the two second law efficiencies as:

$$\eta_{II} = \frac{(P+Q_0/COP_{rev})}{m_{hs}[(h_{hs}^{in}-h_{hs}^{out})-T_0(s_{hs}^{in}-s_{hs}^{out})]} \tag{16}$$

and

$$\eta_{II} = \frac{(P+Q_0)}{m_{hs}[(h_{hs}^{in}-h_0)-T_0(s_{hs}^{in}-s_0)]} \tag{17}$$

where η_{II} is the second law efficiency, P is the net power output, Q_0 is the refrigeration output, COP_{rev} is the coefficient of performance for a reversible (ideal) refrigeration cycle, m_{hs} is the mass flow rate of the heat source fluid, h_{hs}^{in} and h_{hs}^{out} are the inlet and outlet specific enthalpy of the heat source fluid, s_{hs}^{in} and s_{hs}^{out} are the inlet and outlet specific entropy of the heat source fluid, h_0 and s_0 are the specific enthalpy and entropy of the heat source fluid at ambient temperature, and T_0 is the ambient temperature. In the denominator of Eq. (16), the change in exergy of the heat source was used assuming that the heat source fluid is recirculated in a closed loop as in the case of a solar thermal system. However, in Eq. (17) the heat source fluid is assumed to be discharged to the ambient after the heat has been transferred to the working fluid.

In the first definition, Eq. (16), the weight factor used is the reciprocal of the ideal COP ($f=1/COP_{rev}$) which greatly undervalues the refrigeration output. For the second definition, Eq. (17), equal weights were given to both power and refrigeration output ($f=1$). The refrigeration temperature was as low as −68 °C. The first law efficiency (where $f=1$) and second law efficiency, based on Eq. (16), increased initially and then decreased with the refrigeration temperature. At a refrigeration temperature of −28 °C, the first and second law efficiency reached a maximum of 17.4% and 63.7%, respectively. The trend was similar for the turbine inlet pressure, mass fraction of ammonia in the absorber and the refrigeration output of the cycle with the refrigeration temperature using a $1/COP_{rev}$ weight factor for the refrigeration output in the second law efficiency definition. When Eq. (17) is maximized, both first and second law efficiencies drop as the refrigeration temperature decreases.

In order to obtain a simultaneous cooling output a compromise between the work and cooling production exists. For instance, some rectification is needed to produce cooling particularly for a reasonable heat rejection (absorber) temperature such as 35 °C [63]. However, rectification decreases work production because less energy is available (low temperature) and the vapour mass flow rate is lower at the expander inlet. Thus, a new coefficient of performance (effective COP), specific to the Goswami cycle, was proposed to relate the amount of cooling produced with the potential work lost for the combined operation [63,64]. The proposed formulation by Sadrameli and Goswami [64] takes the form:

$$COP_{effective} = \frac{Q_{cool}}{W_{work/opt}-W_{w/cool}} \tag{18}$$

where $COP_{effective}$ is the effective coefficient of performance, Q_{cool} is a cooling heat transfer, $W_{work/opt}$ is ideal work production (optimised using the first law efficiency for work output only by giving no value for cooling) and $W_{w/cool}$ is network output from the cycle in dual output mode. To optimize this trade-off, a thermodynamic analysis has been carried out using the equation-oriented (EO) mode in ASPEN Plus 12.1 [65]. The optimization results confirmed that the conditions for the optimum cooling production are unfavourable for power production. The agreement between the simulation and the experimental results [66] proved that the model developed was accurate. Martin and Goswami [63] evaluated how effective the Goswami cycle was at producing cooling by introducing the effective COP as a new parameter and, therefore, optimizing the gain in the amount of cooling. The maximum overall effective COP of the combined cycle was found to be nearly 1.1 when compared with a work optimised system, which means that for each unit of cooling produced nearly an equal amount of work is generated.

Demirkaya et al. [67] presented a parametric analysis for a Goswami cycle using the ChemCAD process simulator [68]. They studied the performances of the cycle for a wide range of boiler pressures and basic solution ammonia concentrations, and the effects of the sink for rectification cooling, both internal and external, on the cycle output. Using an external source for rectification cooling, is obtained an effective first law and exergy efficiency of 3–5% and 18–28% respectively, with a 50–75% turbine efficiency and, for a boiler and rectifier temperature of 83.4 °C and 41.7 °C, respectively. The effective first law and exergy efficiency could be increased to 3.5–5.5% and 22–33%, respectively, for the same turbine efficiency of 50–75%. The authors claimed that even though the first law efficiency was low, low grade energy (below 100 °C) could be converted into power and refrigeration.

Xu et al. [69] presented a parametric analysis of a Goswami cycle. The simulation studies on this cycle show that the combined cycle achieves a high thermal efficiency of about 23.5% for a heat source temperature of 137 °C, which is higher than the efficiency of the conventional steam power cycle for the same operating conditions. In addition, a system designed to produce 2 MW of electrical power using the cycle will produce more than 700 kW of refrigeration. Using flat-plate or low-concentration solar thermal collectors in this cycle reduced the cost of a solar thermal power plant by 43% in the year 2000.

Pouraghaie et al. [70] optimized the Goswami cycle studied by Xu et al. [69] by varying such design variables as turbine inlet pressure, superheater and condenser temperature. The turbine work, cooling capacity and thermal efficiency of the cycle were

first thermodynamically modelled so that the objective functions could be determined. Finally, the Pareto-based optimization approach was used to find the best possible combination of cycle outputs known as Pareto fronts. The results revealed that two extreme points in the Pareto included those of single-objective optimization results and, therefore, provided more choices for optimal output designs.

A second law analysis was made by Vidal et al. [71] of a combined power and refrigeration cycle proposed by Goswami [72]. The Redlich–Kwong–Soave equation of state was used to calculate the thermodynamic properties of the ammonia–water mixture in the cycle simulation. Both reversible and irreversible cycles were simulated so that the effect of irreversibilities on each component could be studied. The exergy effectiveness was about

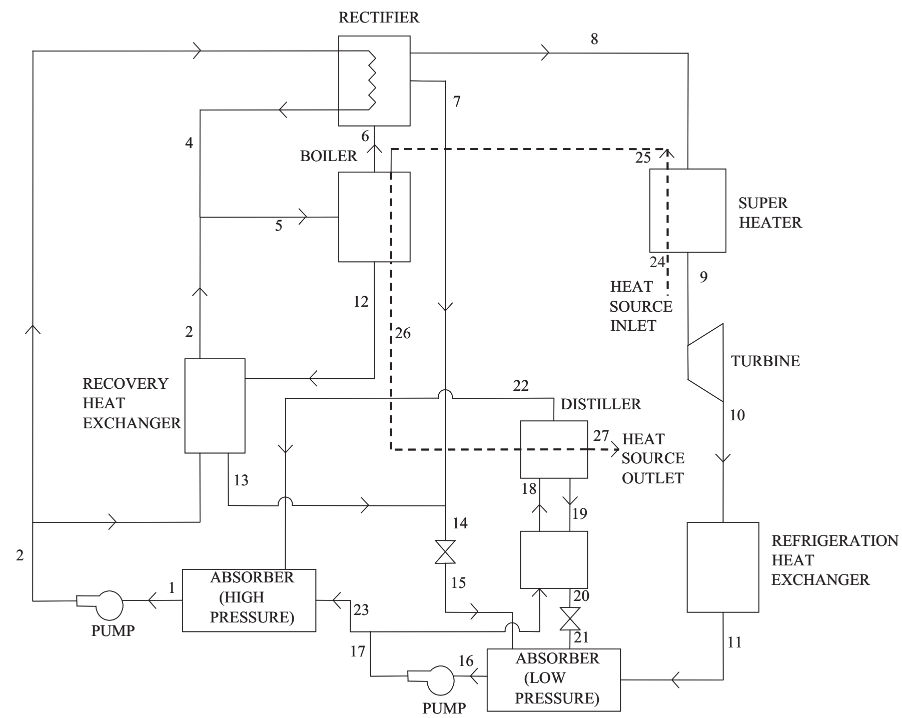


Fig. 6. Modified combined absorption power and cooling cycle—Configuration 1 of Vijayaraghavan and Goswami [73].

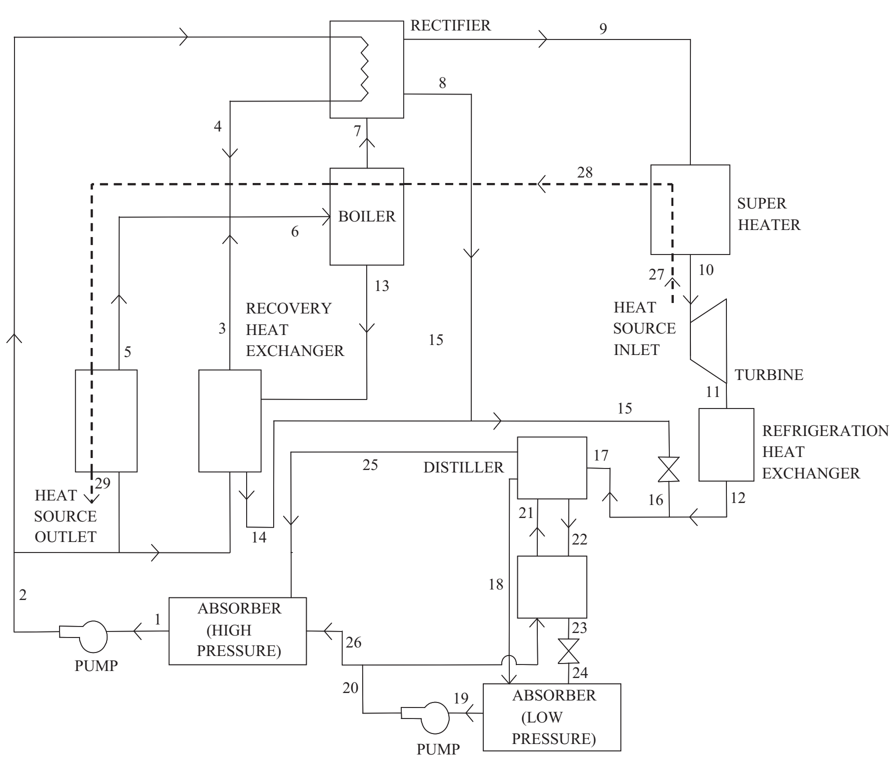


Fig. 7. Modified combined absorption power and cooling cycle—Configuration 2 of Vijayaraghavan and Goswami [73].

53% and 51% for the irreversible cycles when the heat source temperatures were 125 °C and 150 °C, respectively. Even though the amount of cooling produced was less than the amount of power, the second law analysis of the combined cycle shows that both power and cooling can be produced using low-temperature heat sources even for irreversible cycles.

Hasan et al. [72] analysed a combined power and refrigeration cycle proposed by Goswami [58–60] using the first and second laws of thermodynamics. They studied its performance for a heat source temperature range of 57 °C to 197 °C provided by low- and medium-temperature solar collectors. The network output and refrigeration of the cycle, as a percentage of heat input was 16.9% and 1.26%, respectively, giving a first law efficiency of 16.9%. In the first law definition in Eq. (11), the exergy of the cooling effect was used to evaluate the contribution of the cooling output (where $f = 1/COP_{rev}$). The thermodynamic performance of the cycle was optimised for maximum second law efficiency which, according to the definition provided by Eq. (15), was 65.8% and obtained at a heat source temperature of 147 °C. Exergy analysis was performed to determine the losses in the components of the cycle. About 44% of the total irreversibility occurred in the absorber, while the heat recovery in the rectifier and solution heat exchanger accounted for 16% and 24% of the total irreversibility, respectively. Irreversibility in the boiler was high at very low heat source temperatures but dropped at higher temperatures.

Vijayaraghavan and Goswami [73] performed optimisation studies on a Goswami cycle for maximum second law efficiency (known as resource utilization efficiency [RUE]). They performed exergy analysis and the cycle configuration was modified accordingly using a distillation stage (with two different configurations: namely, configurations 1 and 2 [see Figs. 6 and 7, respectively]) to improve the RUE. In the first configuration, a heat source fluid was used for the distillation, while in the second a condensing mixture of weak solution and vapour was used. The first configuration had slightly higher RUE than the second at lower heat source temperatures. The first law efficiency was also higher at optimised RUE conditions. The authors used first law efficiency based on

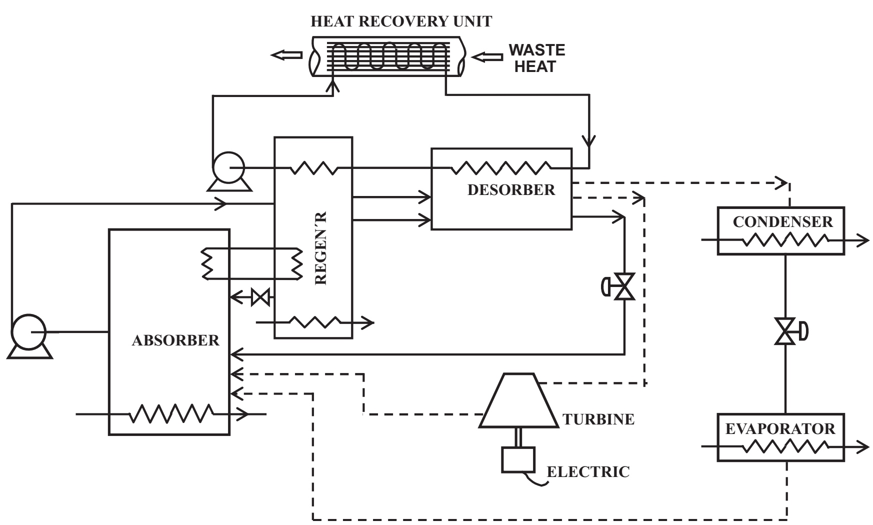


Fig. 8. Flow schematic of the dual-function absorption cycle of Erickson et al. [80].

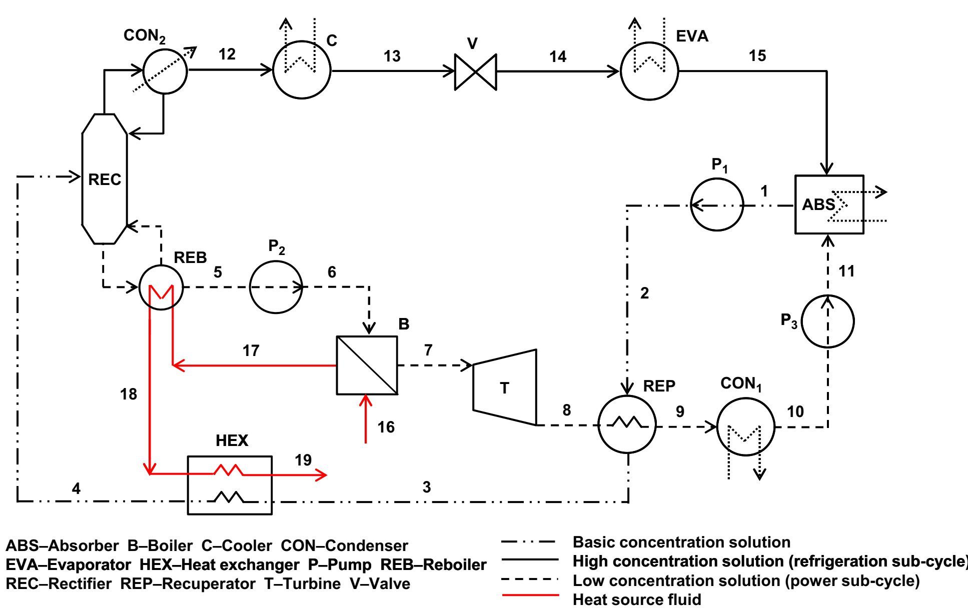


Fig. 9. Schematic diagram for the cogeneration cycle of Zhang et al. [81].

Eq. (11) with a weight factor $1/COP_{rev}$ and also the effective first law efficiency definition described in Eq. (13). The efficiency improved by more than 25% in the modified configurations (configurations 1 and 2). A detailed description of the simulation and optimisation process for the cycle configurations (basic Goswami cycle, modified configurations 1 and 2) can be found elsewhere [74]. The cycle was optimised using a commercially available programme called GRG2, which is one of the variations of the GRG algorithm [75].

Since the Goswami cycle can operate as a bottoming cycle as well as an independent combined power and cooling cycle, Zare et al. [76] carried out a detailed thermodynamic analysis, parametric study, and optimization using the waste heat from a gas turbine-modular helium reactor (GT-MHR) to drive the Goswami cycle. The GT-MHR cycle consists of a compressor, a turbine, a helium reactor, a recuperator and a pre-cooler. They optimized both the combined cogeneration (GT-MHR cycle+Goswami cycle) cycle and GT-MHR power cycle based on the energy utilization (first law) and second law efficiencies. The authors showed that, the power generation and the energy utilization and second law efficiencies of the combined cogeneration cycle were increased with an increase in the turbine inlet temperature. The energy utilization and second law efficiencies of the combined cogeneration cycle were about 9–15% and 4–10% higher than those of the GT-MHR power cycle, respectively at nearly optimum conditions. The parametric study revealed that there is an optimum compressor pressure ratio that maximizes the energy utilization and second law efficiencies of the cycles. At the maximum energy utilization and second law efficiencies the optimum compressor pressure ratio was found slightly higher for the combined cogeneration cycle, which is a disadvantage from economics viewpoint. But, the helium mass flow rate in the combined cogeneration cycle was significantly lower than that in the GT-MHR cycle which can be considered as an advantage economically.

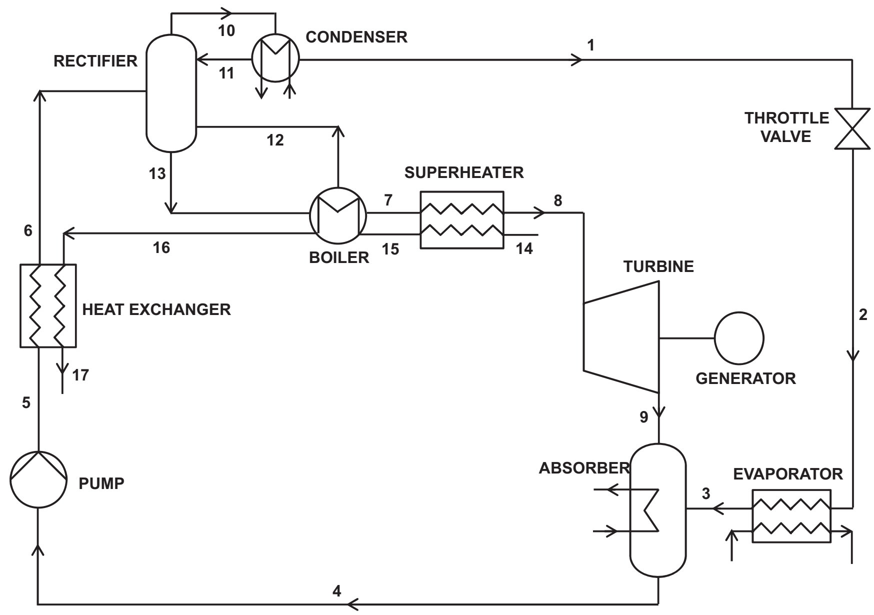


Fig. 10. Schematic diagram of the combined power and refrigeration cycle of Wang et al. [82].

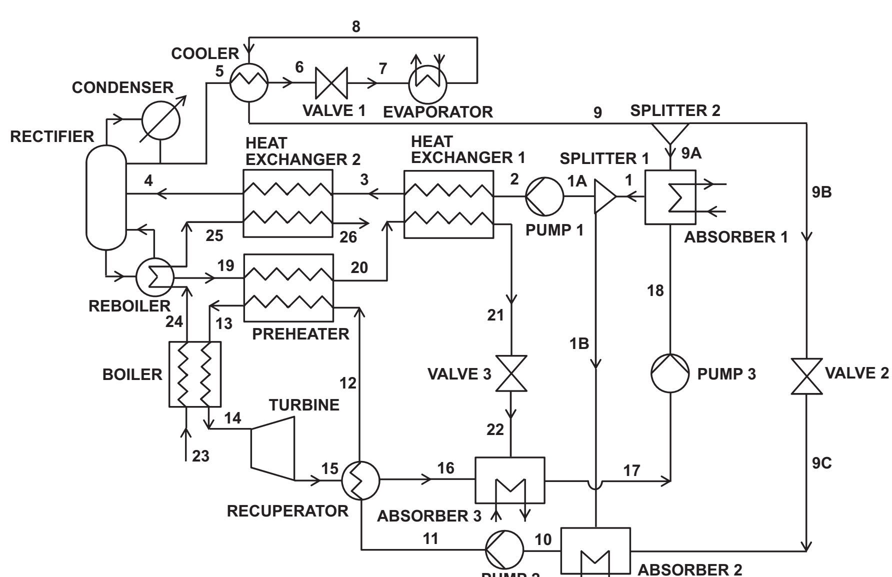


Fig. 11. Flow sheet of the combined power/refrigeration cycle of Liu and Zhang [83].

Moreover, the size of the combined (GT-MHR cycle+Goswami cycle) cycle components is reduced. They also analysed the exergy losses in the different components of the cycles and their results showed that when the GTM-MHR cycle is combined with the Goswami cycle, the exergy losses in the compressor and the turbine increases whereas the exergy losses in the pre-cooler and in the recuperator decrease. The former is due to higher optimum pressure in the combined cogeneration cycle and the latter is due to several reasons such as: a lower temperature difference between the streams, reduced helium mass flow rate, and heat recovery in the boiler and in the superheater of the combined cogeneration cycle.

The Goswami cycle also investigated and optimized from the economic point of view [77]. They applied the genetic algorithm method for conducting the optimization process. Considering a practical range of decision variables, the performance of the cycle is assessed to find out their effects on the thermal and exergy efficiencies as well as on the unit cost of the cycle products (power and cooling). The authors obtained results that show the sum of the unit costs of the products for the cost optimal design is reduced by around 18.6% and 25.9% as compared to that of the thermal efficiency and exergy efficiency optimal designs, respectively. Since the product cost is very low for the cost optimal design case in comparison with other optimal cases (i.e. thermodynamic optimal design cases), they concluded that the cost optimal case is the most promising one at the operating conditions considered in their study. Their result also shows, for each \$3/ton increase in unit cost of the heat source (steam) used, the unit cost of output power and cooling is increased by around \$7.6/GJ and \$15–19/GJ, respectively.

Demirkaya et al. [78], performed a multi-objective thermodynamic optimization study on the Goswami cycle by applying multi-objective genetic algorithms. The network output, cooling capacity, effective first law, and exergy efficiencies of the cycle were considered as objective functions in their Pareto approach optimization of the Goswami cycle. In their study, two case scenarios were analysed. In the first case, the cycle is evaluated as it is a bottoming cycle and in the second case, as it is used as a

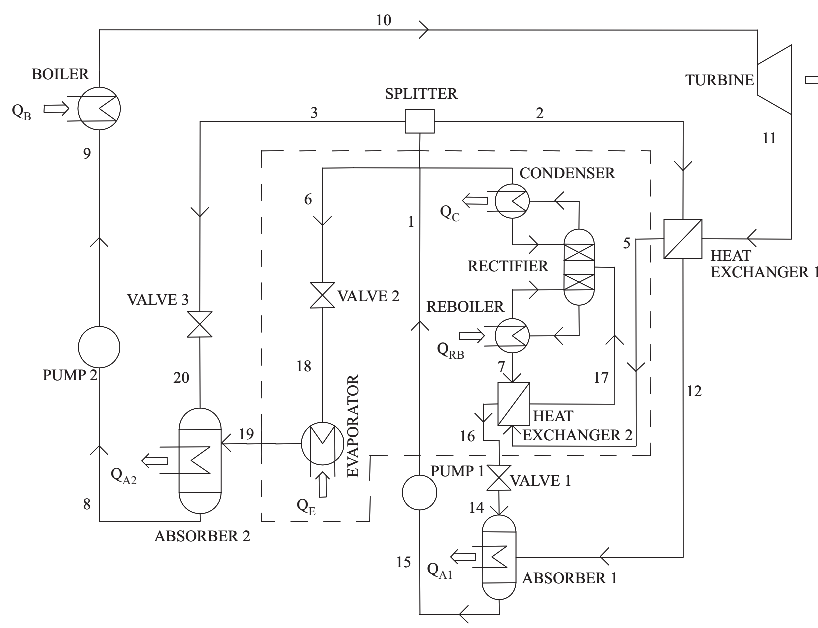


Fig. 12. Absorption combined power/cooling cycle flow scheme of Zheng et al. [84].

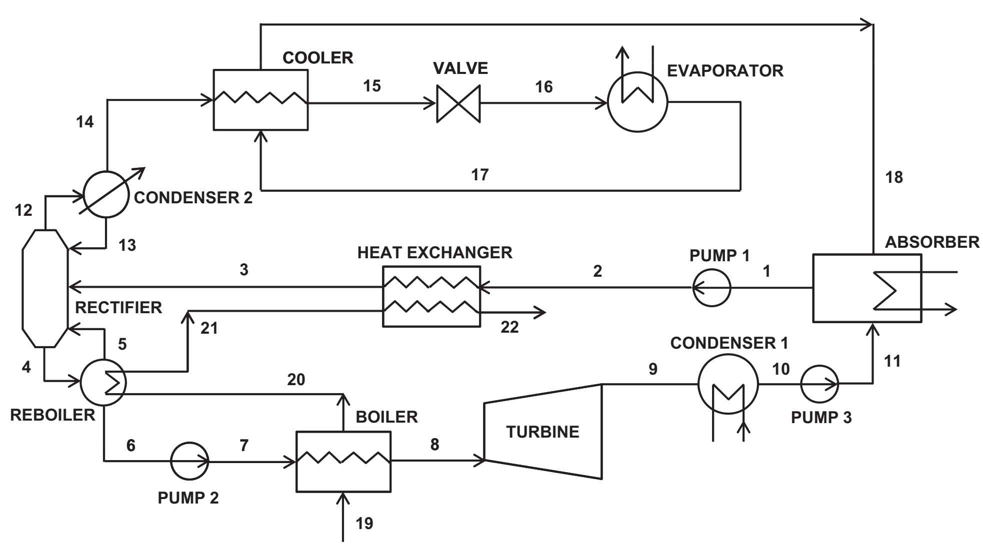


Fig. 13. Flow sheet of the parallel power/refrigeration cycle of Zhang and Lior [85].

top cycle that can utilize energy resources such as solar thermal or geothermal sources as well as waste heat. The optimization is carried out by varying selected design variables as basic solution concentration (between 0.2 and 0.65 ammonia mass fractions), rectifier temperature, and boiler temperature and pressure. The boiler temperature is varied between 70–150 °C and 150–250 °C for the first and second cases considered in the optimization processes, respectively. In the first case (as a bottom cycle), the results of the multi-objective optimization of the four objective functions showed that there is no conflict between network output and exergy efficiency, and improving one results in the improvement of the other one. The maximum values of work and exergy efficiency were attained at the maximum boiler temperature. In the second case (top cycle), the authors showed that there is no conflict between network output, effective first, and exergy efficiencies. The optimal point attained at the maximum boiler temperature and minimum basic solution concentration.

According to the research of Padilla et al. [79], the cost of solar power plants which works normally with Rankine cycles can be reduced by improving the efficiency of the thermodynamic cycle employed in the power plant. The authors proposed a combined Rankine–Goswami cycle (RGC) to improve the efficiency of the power plant, the Goswami cycle with ammonia–water mixture as a working fluid being the bottoming cycle. Using a parabolic trough solar thermal plant with a capacity range of 40 to 50 MW, the performance of the combined RGC under full load conditions and with three different boiler exit case scenarios was

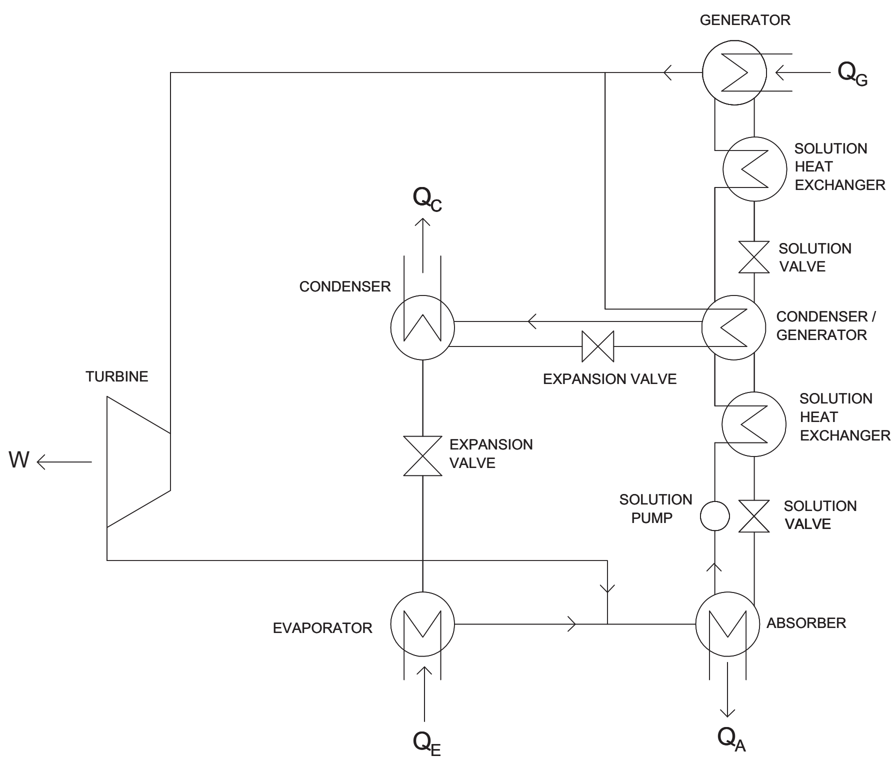


Fig. 14. Double-effect absorption cooling-power plant proposed by Ziegler [15].

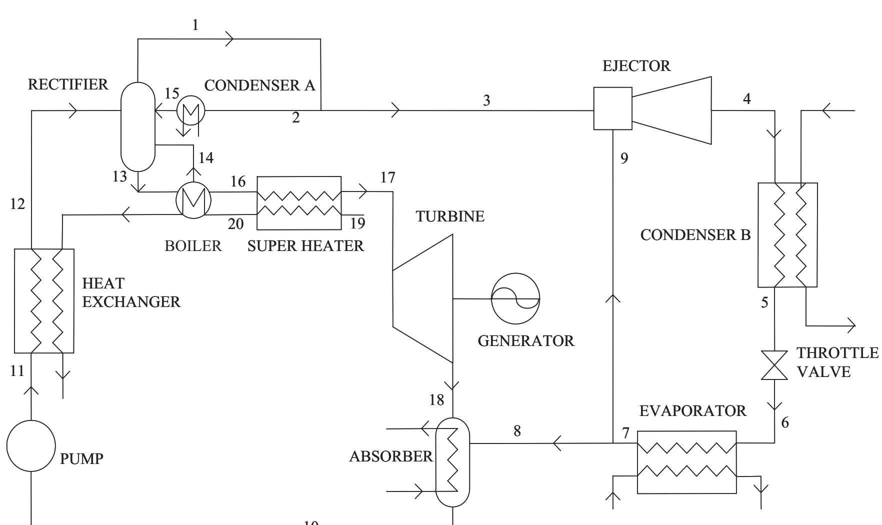


Fig. 15. Schematic diagram of the combined power and ejector absorption refrigeration cycle proposed by Wang et al. [86].

investigated in order to analyse the effects of the ammonia mass fraction, condenser pressure and rectifier concentration on the net power output, cooling, and effective efficiency. The three cases considered are: first case (case R)—the ammonia vapour leaving the boiler is rectified and then expanded in the turbine without superheating; second case (R+S)—in this case a superheater is included in the cycle configuration in order to superheat the rectified vapour before entering the turbine for expansion; the third final case (base case, B)—no superheater or rectification process is used (i.e. the vapour leaving the boiler goes directly for expansion without being superheated or rectified). They found out that as the condenser pressure increases (between 0.2 to 9 bar), the network output goes up to a maximum value (57 MW) and then decreases for the case R and case (R+S). However, for the base case (B) as the condenser pressure increases the net power output increases too with the

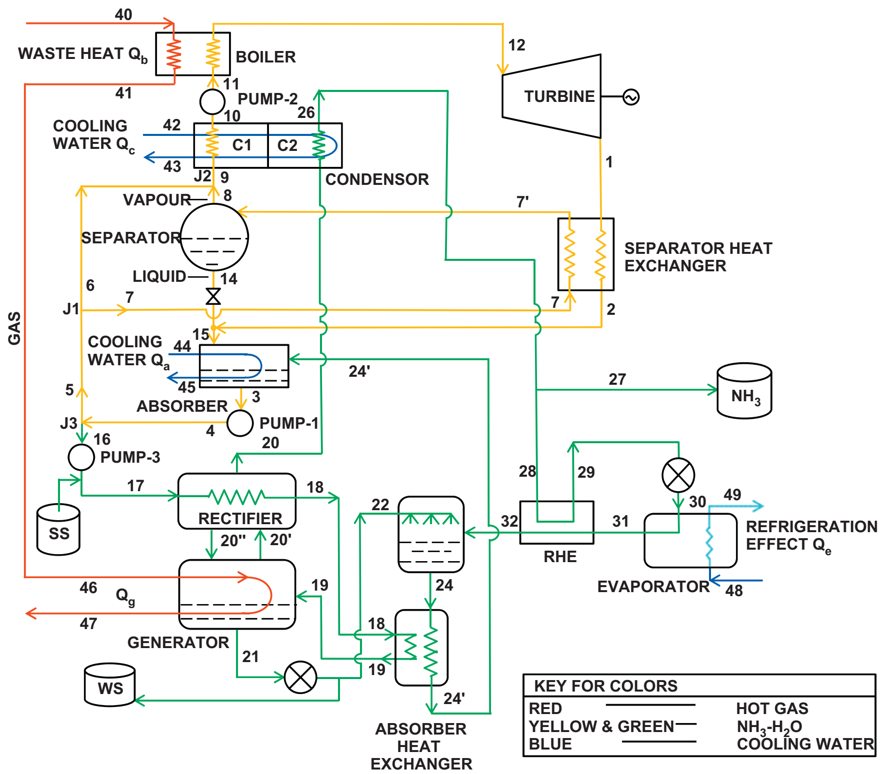


Fig. 16. Flow diagram of the complete LHECUS cycle proposed by Kiani et al. [87].

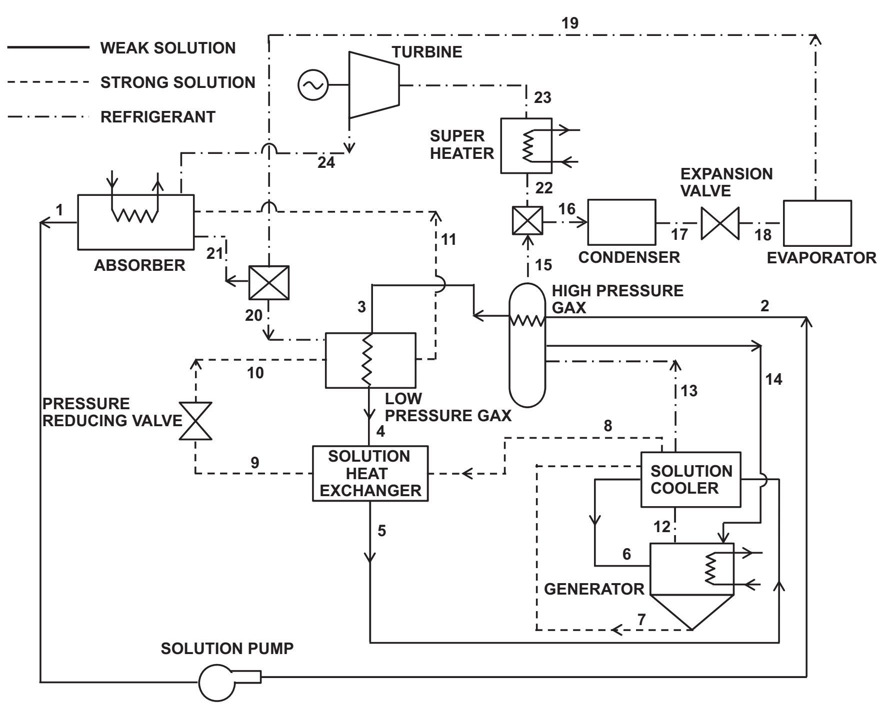


Fig. 17. Schematic diagram of GAX based absorption cooling and power cycle [91].

highest network output value of 85 MW. For the range of condenser pressure between 3.5 and 9.0 bar, the cooling capacity of the cycle configuration with a rectifier (case R) is highly sensitive to the ammonia mass fraction. For base case (B), the first law efficiency values were in the range of 29.4%–36.7% while that for cases R and R+S in the range of 19.2%–33.3%.

4.2. Other ammonia–water cycle configurations

Using ammonia–water as the working fluid, several researchers have proposed new cycle configurations for dual function (power and cold production). These cycles are reviewed in this subsection.

Erickson et al. [80] proposed an ammonia–water absorption cycle configuration that produces power and refrigeration interchangeably. The dual function absorption cycle is capable of converting low temperature (< 300 °C) sensible heat into power and refrigeration. Fig. 8 shows a simplified flow schematic of the cycle. It consists of a heat recovery unit, desorber, recuperator, absorber, turbine with electric generator, condenser and evaporator. The power and absorption cycle use the same absorption unit to improve the economics of recovering low-grade energy.

Zhang et al. [81] proposed a new ammonia–water system (see Fig. 9) for the cogeneration of power and refrigeration. The system operates in a parallel combined mode with an ammonia–water Rankine cycle and an ammonia refrigeration cycle, interconnected by absorption, separation and heat transfer processes. The authors found that the cycle has a good thermal performance with energy and exergy efficiencies of 25% and 50.9%, respectively, for the base case considered. The comparison between the cycle and the separate generation of power and refrigeration showed that the new cycle has the advantage that it consumes less energy (21.6% less). Wang et al. [82] studied the performance of a combined refrigeration and power cycle (Fig. 10), driven by waste heat but which can be heated by any heat source (e.g. solar energy, geothermal heat or an exhaust flue gas from a gas turbine). This cycle configuration is a modification of the cycle proposed by Zhang et al. [81]. The major difference between the two cycles is that the feed pump and condenser have been removed before and after the turbine in the cycle proposed, which makes the cycle simpler and less costly. A detailed parametric analysis was carried out to study the effect of such parameters as heat source temperature, refrigeration temperature, ambient temperature, turbine inlet pressure and basic solution ammonia mass fraction on the performance of the combined (dual-function) cycle. The authors optimised the thermal parameters in the cycle using the exergy efficiency as an objective function and the genetic algorithm method. The optimised exergy efficiency was 43% for a given condition.

Liu and Zhang [83] proposed a novel ammonia–water combined cycle for the cogeneration of power and refrigeration. As shown in Fig. 11, a splitting/absorption unit was introduced into the combination of an ammonia–water Rankine sub-cycle and an ammonia refrigeration sub-cycle. The condenser in the Rankine cycle was replaced by an absorber. In this configuration, the basic solution of ammonia–water is separated into a high concentration ammonia vapour and a relatively weak solution liquid in a device that operates like a distillation column. The modifications increased the ammonia mass fraction in the heat addition process and reduced it in the absorption–condensation process. The performance of the cycle was evaluated by exergy efficiency and found to be 58% for the base case studied. The cogeneration unit used nearly 18% less energy than the conventional separate system of power generation (a steam Rankine cycle) and refrigeration (an ammonia–water absorption refrigeration cycle). The authors also suggested that there is an optimum pair of two split fractions: namely, SF1 (the ratio of the mass flow rate of the basic concentration solution split to heat exchanger 1 to the total mass flow rate of the basic concentration solution) and SF2 (the ratio of the mass flow rate of the high concentration solution split to absorber 1 to the total mass flow rate of the high concentration solution from the cooler) at which the exergy efficiency was maximum.

Zheng et al. [84] proposed a combined power and cooling system (see Fig. 12) in which the flash tank or separator in the Kalina cycle was replaced by a rectifier to enhance the separation process and to obtain an additional higher purity stream of ammonia for cooling. In order to produce a larger refrigeration output, the fluid should go through a phase change in the cooler. The proposed cycle requires two absorbers and was modelled with the process simulator Aspen Plus. A condenser and an evaporator were introduced between the rectifier and the second absorber. With these modifications, the cycle can simultaneously

Table 2
Operating condition for other ammonia–water combined absorption power and cooling cycles found in the literature.

Reference	Cycle description	Temperature (°C)			Turbine Parameter		
		Heat source (Inlet)	Sink	Refrigeration	η_t (%)	Inlet/Outlet Pressure (bar)	Inlet/Outlet Temperature (°C)
Erickson et al. [80]	GAX+ARC	175	15[a]	N.A	75	25.1/5.2	155.0/61.7
Zhang et al. [81]	Rankine+ARC	465	30[a]	0.0	87	50.0/0.376	450.0/70.1
Wang et al. [82]	Rankine+ARC	300	20[b]	−5.0	85	25.0/1.194	285.0/96.9
Liu et al. [83]	Rankine+ARC	465	30[a]	−15.0	87	111.0/0.39	450.0/68.0
Zheng et al. [84]	Kalina+ARC	350[c] and 135[d]	35	−10.0	N.A	49.0/0.981	350/84.5
Zhang et al. [85]	Rankine+ARC	465	30[a]	−15.0[e]	87	51.0[f]/0.191[f], 152.5[g]/0.853[g] 75.8[h]/0.191[h] and 0.40[h]	450.0[f]/56.7[f], 450.0[g]/83.6[g] 450.0[h]/56.6[h] and 66.8[h]
Wang et al. [86]	Rankine+ Ejector- ARC	300	20[b]	−5.0	85	25.0/1.194	285.0/96.9
Kiani et al. [87]	Kalina+ARC	520	20[b]	7.0[i]	90	115.0/5.46	510.0/190.2
Zhang et al. [88]	Rankine+ARC	465	30[a]	−11.4[e]	87	52.4/0.242	450.0/61.3

ARC—Absorption Refrigeration Cycle; η_t—Isentropic turbine efficiency

[a] External cooling water inlet temperature
[b] Ambient
[c] Boiler input temperature
[d] Reboiler input temperature
[e] Evaporator outlet temperature; N.A—Not available
[f] Parallel cogeneration system
[g] Series connected cogeneration system ($SF_1=0.4$)
[h] Compound configuration system ($SF_2=0.72$)
[i] External chilled water outlet temperature

provide refrigeration and generate power. The overall thermal efficiency and exergy efficiency of the proposed cycle were found to be 24.2% and 37.3%, respectively. The addition of refrigeration as a useful output not only improves cycle performance, but expands the application flexibility of the system.

Zhang and Lior [85] suggested that, by adding a rectifier, the liquid ammonia-water stream could be evaporated and superheated in the reboiler at the bottom of the rectification column and later expanded in the turbine. The authors developed three different configurations: namely, parallel, series and compound cogeneration cycle configurations for the integration of refrigeration and power generation systems with a single heat source using ammonia–water as the working fluid. The heat source fluid used was air. In the configurations analysed, the energy and exergy efficiencies were found to be 26% to 28% and 55% to 60%, respectively, at a heat input temperature of 450 °C. The parallel cycle configuration shown in Fig. 13 had the highest refrigeration to power ratio (0.37), while the compound configuration had the lowest (0.25). For a constant flow rate of the heating fluid, the compound configuration produced 9% and 11% more power, and 28% and 11% less refrigeration, respectively, than the parallel and series cycle configurations. When the heat source used was exhaust from the gas turbine plants, the total plant energy efficiency increased to 57%. These cycles has resulted in a potential high capital investment. Moreover, these cycles require high driving temperatures and therefore cannot be combined with solar energy for small- and medium-scale applications.

Table 3
Efficiencies and power to cooling ratio for different types of combined absorption power and cooling cycle.

Reference	Efficiency (%)		Power/ cooling ratio	Remark
	Thermal	Exergy		
Erickson et al. [80]	11.96	N.A	N.A	• Turbine power output, $P=1.77\ MW_e$; • When $P=0$, refrigeration output, $Q_o=10.5$ MW
Zhang et al. [81]	25.00	50.90*/ 53.40**	4.00	• For the base case considered; • Energy efficiency weighs both power and cooling equally ($f=1$); • For exergy efficiency: - $f=1/COP_{rev}$ (*) - $f=1/COP_{practical}$ (**), $\eta_{ref}=40\%$
Wang et al. [82]	20.45	35.54	2.73	• For a particular operating condition; • For optimised condition: - Power to cooling ratio=4.24 and $\eta_{ex}=43\%$; • Thermal efficiency weighs both outputs equally ($f=1$); • Exergy efficiency based on $f=1/COP_{rev}$
Liu et al. [83]	N.A	57.60	3.62	• Performance parameters for the base case; • Exergy efficiency based on $f=1/COP_{rev}$
Zheng et al. [84]	24.20	37.30	2.48	• Overall thermal efficiency weighs power and refrigeration effect equally ($f=1$); • Exergy efficiency weighs the refrigeration output by factor $f=1/COP_{rev}$
Zhang et al. [85]	28.20[a]/ 26.42[b]/ 27.92[c]	55.80[a]/ 54.12[b]/ 59.50[c]	2.70[a]/ 3.27[b]/ 4.08[c]	• Three cycle configurations analysed at the base case; • The energy efficiency equally weighs the power and refrigeration outputs ($f=1$); • Exergy efficiency based on $f=1/COP_{rev}$
Wang et al. [86]	20.97	35.77	2.49	• The performance parameters were for a particular operating condition; • Parametric analysis were done; • Thermal efficiency weighs both power and refrigeration output equally ($f=1$); • Exergy efficiency based on $f=1/COP_{rev}$
Kiani et al. [87]	30.00	N.A	N.A	• Maximum overall thermal efficiency of the hybrid cycle based on $f=1/COP_{practical}$ where $COP_{practical}=2.48$
Zhang et al. [88]	27.70	55.70	2.99	• Performance parameters were determined for the base case; • Energy efficiency weighs the power and refrigeration outputs equally ($f=1$); • Exergy efficiency based on $f=1/COP_{rev}$
Jawahar et al. [91]	35.00–45.00	N.A	0.36***	• Maximum overall thermal efficiency of the combined cycle based on $f=1$; • (***)—at $t_G=150$ °C, $t_{sink}=35$ °C, $t_E=0$ °C, optimum split factor (0.8) and split ratio (0.5). • $COP=0.35$ at the optimum condition

N.A—Not Available; η_{ref}—Second law efficiency of refrigeration

[a] Parallel cogeneration system
[b] Series connected cogeneration system ($SF_1=0.4$)
[c] Compound configuration system ($SF_2=0.72$)

A modified form of the basic absorption cooling cycle has been presented by Ziegler [15]. Fig. 14 shows a cooling and power cycle derived from a double-effect absorption system. It is estimated that with this cycle configuration 1.2 MW of cooling and 100 kW of power can be produced from 1 MW of thermal energy when the system operates as a pure chiller and pure sorption power cycle, respectively. The main advantage of these configurations is that low-grade heat (such as solar energy or waste heat) can be used and the ratio between cold and power production can be adjusted.

A new combined power and ejector-absorption refrigeration cycle that can be operated by solar, geothermal and industrial waste heat has been proposed by Wang et al. [86]. The proposed cycle (see Fig. 15) originated from the cycle developed by Wang et al. [82] and introduces an ejector between the rectifier and the condenser. The high-pressure ammonia-rich vapour from the rectifier is used as the primary flow entering the ejector, and entrains low-pressure ammonia-rich vapour from the evaporator. As a result of introducing the ejector, the refrigeration capacity can be increased without significantly increasing the capacities of the rectifier and absorber. For instance, in comparison with the cycle in Ref. [82] the refrigeration capacity of the cycle with the ejector increased by 9.5% under the same conditions. Thus, the combined cycle can improve the cycle performance without greatly increasing the complexity of the system. Such parameters as heat source temperature, condenser temperature, evaporator temperature, turbine inlet pressure, turbine inlet temperature, and basic solution ammonia concentration have significant effects on the net power output, refrigeration output and exergy efficiency of the combined cycle.

The load-leveling hyper energy converting and utilization system (LHECUS) is a hybrid cycle which uses ammonia–water as the working fluid in a combined power generation and refrigeration cycle developed by Kiani et al. [87]. The power generation cycle functions as a Kalina cycle and it is combined with an absorption refrigeration cycle as a bottoming cycle. Fig. 16 shows the flow diagram of the complete cycle configuration. LHECUS is designed to utilize the waste heat from industry to produce cooling and power simultaneously. The refrigeration effect can be either transported to end-use sectors by means of a solution transportation absorption chiller (STA) driven by solution concentration difference or stored for demand load levelling.

Zhang and Lior [88] proposed a new ammonia–water system for the cogeneration of refrigeration and power. The plant is a parallel combination between an ammonia–water Rankine cycle and an ammonia refrigeration cycle interconnected by absorption, separation and heat transfer processes. The authors investigated the effects of such key thermodynamic parameters as basic working solution concentration, the cooling water temperature, and turbine inlet parameters on both energy and exergy efficiencies. In the base-case studied, the cycle has energy and exergy efficiencies of 27.7% and 55.7%, respectively. The cycle requires a high temperature (450 °C) at the superheater, which makes the cycle unfavourable for small- and medium-scale applications driven by low-grade thermal energy.

As the GAX cycle has shown promising results in enhancing the performance of absorption cooling systems [89,90], a new absorption cooling and power cycle using a GAX has been proposed (see Fig. 17) [91]. The GAX based power and cooling cycle is a modification of the simple absorption power and cooling cycle configuration. The thermodynamic analysis of the cycle was carried out for different generator, sink and evaporator temperatures. The split ratio (refrigerant flow ratio between power and cooling systems) was also varied in the analysis. The extent to which the COP and thermal efficiency of the GAX cycle varied with respect to the split factor (solution flow ratio between absorber and GAX heat exchanger) at a fixed split ratio (0.5) was studied for a constant heat source and sink temperature. The optimum value for the split ratio was found to be 0.5 and the optimum split factor 0.8–0.9. At the optimum split ratio the cooling capacity and power output of the cycle was 225 kW and 80 kW, respectively, for generator, sink and evaporator temperatures of 150 °C, 35 °C and 0 °C. The combined thermal efficiency and COP in the optimum operating conditions were 35–45% and 0.35, respectively.

The cycle configurations reviewed above are summarised in Table 2 with heat source inlet, sink and refrigeration temperatures. Other parameters such as turbine inlet and outlet temperatures and pressures are also given in Table 2. The performance parameters of the combined cycle configurations such as power-to-cooling ratio, and thermal (energy) and exergy efficiencies of the cycles are presented in Table 3.

4.3. Property database effect on the cycle performance analysis

To demonstrate the influence of the ammonia–water property database source on the analysis of a combined power and cooling cycle, a well-known combined power and cooling cycle (Goswami cycle) was selected. The input parameters and the model assumptions considered in the analysis of the cycle illustrated in Fig. 5 were shown in Table 4. The cycle simulation was conducted under the following conditions:

- Steady-state steady flow operation;
- Thermal and pressure losses were neglected;
- Throttling valve was isenthalpic;
- Saturated basic solution stream leaving the absorber at the absorber pressure;

Table 4
Input parameters and main assumptions considered for cycle analysis (Fig. 5).

Parameter	Value
Reference temperature (°C)	17.0
Desorber temperature (°C)	125.0
Desorber pressure (bar)	20.5
Absorber pressure (bar)	1.5
Basic solution concentration (ammonia mass fraction)	0.43
Rectifier temperature (°C)	108.5
Expander isentropic efficiency (%)	85
Pump isentropic efficiency (%)	80
Second law efficiency of refrigeration (%)	30
Minimum temperature difference for each heat exchanger (°C)	5.0
Mass flow rate of basic solution (basis for calculation, kg/s)	1.0

Table 5
Effect of ammonia-water mixture database on cycle parameters calculation.

Cycle parameter	Ammonia–water database			
	(I)	(II)	(III)	(IV)
Turbine power (kW)	44.00	47.81	47.96	52.60
Pump power (kW)	2.78	3.07	3.00	3.00
Boiler heat duty (kW)	271.70	294.00	321.44	324.50
Absorber heat duty (kW)	233.90	252.00	279.81	277.00
Cooling load (kW)	3.35	2.77	3.85	4.00
Cooling to power ratio, r	0.081	0.062	0.086	0.081
Effective first law efficiency (%), [67]	15.1	15.2	14.0	15.3

(I)—Ibrahim and Klein [32]; (II)—Tillner-Roth and Friend [41]; (III)—PSRK equation of state and Latent-heat H model used [67]; and (IV)—SRK equation of state used [67].

- Saturated liquid and vapour streams leaving the desorber are in equilibrium at the desorber temperature and pressure;
- No superheater was considered;
- Saturated liquid and vapour streams leaving the rectifier are in equilibrium at the rectifier temperature and pressure;
- Water was used as a chilled fluid in the refrigeration heat exchanger.

The results of the cycle calculations are presented in Table 5. The turbine power shows a relative difference of about 16.4%, from the lowest 44.0 kW (I) to the highest 52.6 kW (IV). In the other cycle components, relative differences between the highest and lowest values of heat duty were about 9.4%, 16.4%, 16.4% and 30.8% for the pump, boiler, absorber and refrigeration heat exchanger, respectively. The reason for these discrepancies is that different property databases (equation of states) were used in the analysis.

Hence, the appropriate thermophysical property data need to be used to analyse combined absorption power and cooling systems and care must be taken to avoid confusion when projections based on different databases are used. Of the sources analysed, the property data correlation evaluated by Tillner-Roth and Friend [41] seems to predict the experimental values with reasonable accuracy. NIST REFPROP 9 [92] includes the correlation proposed by Tillner-Roth and Friend [41] to predict the ammonia–water mixture properties. The combination of experimental uncertainties and database deviations may make it difficult to interpret energy and mass balance calculations performed in cycle analysis.

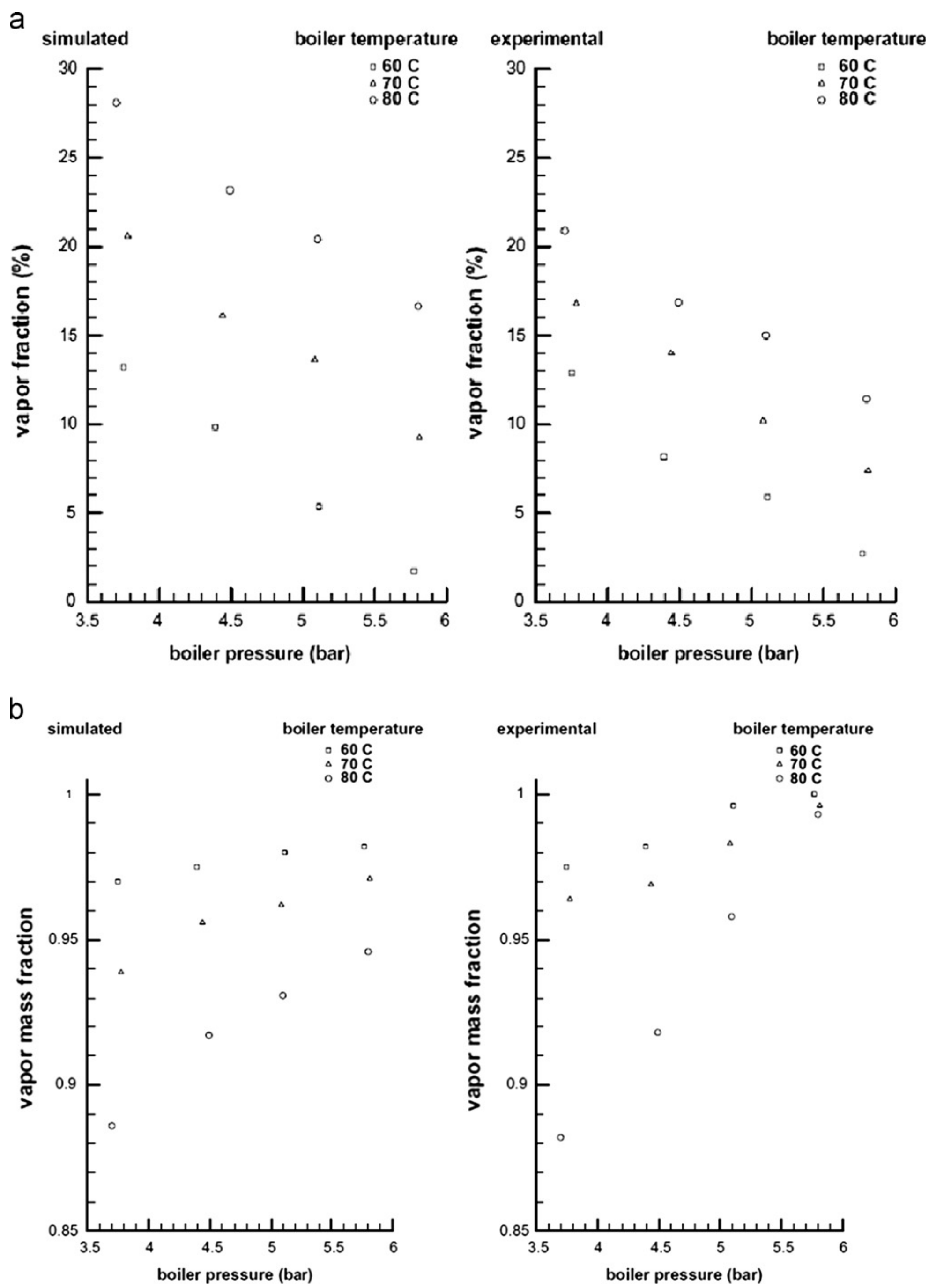


Fig. 18. (a) Vapour fraction for various boiler temperatures and pressures [93] and (b) vapour mass fraction for various boiler temperatures and pressures [93].

Experimental work on combined absorption power and cooling systems is very limited and will be presented in the next section.

4.4. Experimental studies

The experimental work published on the feasibility, operating conditions and processes involved in combined absorption power and cooling cycles is based on the Goswami cycle configuration. The studies were made using the laboratory experimental setups at the University of Florida, USA.

The Goswami cycle was theoretically and experimentally investigated by Tamm et al. [93,94]. The parametric studies revealed that the cycle can be optimized for first and second law efficiency as well as power and cooling output. The thermal efficiency, and the power and the cooling outputs decrease by 20.6%, 11.8% and 37.7% respectively when the real losses are considered in the analysis. The theoretical analysis showed that when the cycle is optimised for second law efficiency, it produces no refrigeration at high heat source temperatures, but it does have a refrigerating effect at low heat source temperatures. The experimental studies demonstrated the feasibility of a combined power and cooling cycle. The results of the experiments confirmed that the vapour production and absorption–condensation processes work well. The agreement between the theoretical and experimental results was found to be close (Fig. 18a and b).

Martin [66] made an experimental study on the novel concept of producing power and cooling using low temperature ($<200\,^{\circ}C$) thermal resources. The experimental setup developed by Martin was based on Tamm [95] but included a rectifier and a turbine to condition the vapour and to extract work from the fluid, respectively, with the aim of demonstrating the sub-ambient turbine exhaust conditions. The author concluded that with better expander performance, practical power and cooling production can be achieved with the proposed novel cycle (Goswami cycle). Subsequently, Goel [96] studied the absorption and condensation process by modifying the rectifier column (increasing its diameter from 2 to 3 in.) and making the separator vessel smaller. The study proposed a new concept that enhances heat and mass transfer processes in a falling film absorber and considerably reduces the absorber size without having any effect on high vapour and coolant side pressure drops. After the experiments performed by Goel, all the components in the setup were upgraded and replaced (including the expansion device, which is replaced by scroll type expander) except the separator and the rectifier column [97]. The scroll expander isentropic efficiency was between 30–50%, and the expander performed better when the vapour was superheated [97].

The selection of a suitable expansion device is crucial for power generating systems. For large scale power generating systems (in MW), steam turbines (turbo type expanders) are well established technologies [97]. However, for small and medium scale applications for instance for buildings the development of a suitable expansion device is necessary in particular for expanders working with ammonia. This is mainly due to the following two main reasons: first it is difficult to find an off-the-shelf expander with high efficiency for such type of applications; second ammonia is corrosive to copper and copper containing alloys therefore it presents a limitation on the selection and design of expanders. Scroll expanders (volumetric type expanders) are one of the candidates for small-medium size capacity applications. The use of organic rankine cycles (ORCs) allows the conversion of low-grade heat sources such as geothermal, solar thermal, industrial waste heat, etc into mechanical or electrical power [98]. Several researchers suggested and have done experimental and numerical studies on the use of scroll expanders for ORCs [99–101]. Since custom design and fabrication of scroll expander can be costly, they used commercially available scroll compressors by modifying it to work as expander.

5. Conclusion

The increasing consumption of fossil fuels has resulted in such environmental issues as ozone depletion, global warming and atmospheric pollution. In order to save energy and to protect the environment, it has become extremely important to use environmentally friendly working fluids and low-grade energy sources such as industrial waste heat, biomass, solar and geothermal energy, etc. The working fluid that has been proposed for a combined absorption power and cooling cycle is a binary mixture of ammonia–water, which is environmentally friendly.

A wide variety of cycle configurations has been studied and reported in the literature. The literature on the combined absorption power and cooling cycles has found that greater importance is given to power output than cooling. Two general types of cycles have been identified: those producing cooling using sensible heat (mainly the Goswami cycle) and those based on latent heat (mainly hybrid Rankine and absorption chiller cycles).

This paper has presented an overview of the existing combined absorption power and cooling cycles. Some of the configurations are simple modifications of the Kalina absorption power cycle that produce cooling as a sub product. In some cases these cycles are very complex and have a high number of splits and components or require very high driving temperatures (Table 2). The most suitable combined absorption power and cooling systems for solar applications in buildings seem to be those derived directly from such absorption chiller cycles as single- or double-effect cycles or advanced GAX cycles. These systems will help to overcome such technological challenges as the development of suitable expanders for small-medium capacity solar applications.

More experimental investigations are essential if cycle performances are to be compared in detail. As research in this field has just started, a considerable amount of work still has to be done before combined absorption power and cooling cycle technology can play a major role in the future.

Acknowledgements

The authors acknowledge the support of the Spanish Ministry of Economy and Competitiveness (ENE2009-14177) and the Catalan Government (2009SGR-33). Dereje S. Ayou thanks the AGAUR (Catalan Government) for a fellowship.

References

[1] Europe in figures—Eurostat yearbook: 2011 Energy, 〈http://epp.eurostat.ec.europa.eu〉; 2011.
[2] Bertoldi P, Atanasiu B. Electricity consumption and efficiency trends in European Union—status report. JRC scientific and technical reports. JRC53919; 2009.
[3] Henning HM. Overview on Solar Cooling. In: Proceedings of the 3rd european solar thermal energy conference, ESTEC 2007. Freiburg, Germany; 2007.
[4] Styliaras VE. A freon-ammonia comparison applied in a mixed power cycle. Heat Recovery Systems & CHP 1995;15(6):601–3.
[5] Kalina AI. Combined-cycle system with novel bottoming cycle. ASME paper: 84-GT-173; 1984.
[6] Vijayaraghavan S, Goswami DY. Organic working fluids for a combined power and cooling cycle. Journal of Energy Resources Technology. Transactions of the ASME 2005;127:125–30.
[7] Maloney JD, Robertson RC. Thermodynamic study of heat power cycles. Oak Ridge National Laboratory Report. CF-53-8-43; 1953.
[8] Kalina AI. Combined cycle and waste-heat recovery power systems based on a novel thermodynamic energy cycle utilizing low-temperature heat for power generation. ASME paper: 83-JPGC-GT-3; 1983.

[9] Ogriseck S. Integration of Kalina cycle in a combined heat and power plant, a case study. Applied Thermal Engineering 2009;29(14–15):2843–8.
[10] Kalina AI, Leibowitz HM. System design and experimental development of the kalina cycle technology. In: Proceedings from the ninth annual industrial energy technology conference: ESL-IE-87-09-44. Houston, TX; September 16–18, 1987.
[11] Madhawa HD, Golubovic M, Worek WM, Ikegami Y. The performance of the kalina cycle system 11 (KCS-11) with low-temperature heat sources. Journal of Energy Resources Technology 2007;129:243–7.
[12] Desideri U, Bidini G. Study of possible optimisation criteria for geothermal power plants. Energy Conversion and Management 1997;38(15–17): 1681–91.
[13] Nasruddin R, Rifaldi M, Noor A. Energy and exergy analysis of kalina cycle system (KCS) 34 with mass fraction ammonia-water mixture variation. Journal of Mechanical Science and Technology 2009;23(7):1871–6.
[14] Wasabi Energy Ltd. Announcement: Wasabi Energy subsidiaries secure contract with FLSmidth to build 8600 kW Kalina Cycle® Power Plant. 〈http://www.wasabienergy.com〉; 2011.
[15] Ziegler F. Novel cycles for power and refrigeration. In: Proceedings of the 1st european conference on polygeneration. Tarragona, Spain; 2007.
[16] Vijayaraghavan S, Goswami DY. On evaluating efficiency of a combined power and cooling cycle. Journal of Energy Resources Technology 2003;125:221–7.
[17] Lior N, Zhang N. Energy, exergy, and second law performance criteria. Energy 2007;32(4):281–96.
[18] Ibrahim OM, Klein SA. Absorption power cycles. Energy 1996;21(1):21–7.
[19] Amano Y, Suzuki T, Hashizume T, Akiba M, Tanzawa Y, Usui A. A hybrid power generation and refrigeration cycle with ammonia–water mixture. In: Proceedings of the international joint power generation conference, Florida, USA; 2000. p. 1–6.
[20] Dejfors S, Thorin E, Svedberg G. Ammonia–water power cycles for direct fired cogeneration applications. Energy Conversion and Management 1998;39(16–18):1675–81.
[21] Rogdakis ED, Antonopoulos KA. A high efficiency NH_3/H_2O absorption power cycle. Heat Recovery Systems & CHP 1991;11(4):263–75.
[22] Hassani V, Dickens J, Parent Y. Ammonia/water condensation test: plate fin heat exchanger (absorber/cooler). NREL, Golden CO; September, 2001.
[23] Jonsson M. Advanced power cycles with mixtures as working fluid. PhD thesis. RIT, Stockholm, Sweden; 2003.
[24] Jonsson M, Thorin E, Svedberg G. Gas engine bottoming cycles with ammonia-water mixtures as working fluid. In: Proceedings of the world energy research symposium. Florence, Italy; 1994, p. 1–11.
[25] Kalina AI, Leibowitz HM. Application of the Kalina cycle technology to geothermal power generation. Geothermal Resources Council Transactions 1989;13:605–11.
[26] Olsson EK, Thorin EB, Dejfors AS, Svedberg G. Kalina cycles for power generation from industrial waste heat. In: Proceedings of the world energy research symposium. Florence, Italy; 1994, p. 39–49.
[27] Park YM, Sonntag RE. A preliminary study of the Kalina power cycle in connection with a combined cycle system. International Journal of Energy Research 1990;14(2):153–62.
[28] Thorin E. Power cycles with ammonia–water mixtures as working fluid. Analysis of different applications and the influence of thermophysical properties. PhD thesis. RIT, Stockholm, Sweden; 2000.
[29] Jonsson M, Yan J. Exergy and pinch analysis of diesel engine bottoming cycles with ammonia–water mixtures as working fluid. International Journal of Applied Thermodynamics 2000;3(2):57–71.
[30] Marston CH, Hyre M. Gas turbine bottoming cycles: triple-pressure steam versus Kalina. Transactions of the ASME 1995;11:110–5.
[31] El-Sayed YM, Tribus M. Thermodynamic properties of water–ammonia mixtures: theoretical implementation for use in power cycles analysis, vol. 1. New York: AES ASME; 1985 p. 89–95.
[32] Ibrahim OM, Klein SA. Thermodynamic properties of ammonia–water mixtures. ASHRAE Transactions Symposia 1993;99(1):1495–502.
[33] Park YM. A Generalized equation of state approach to the thermodynamic properties of ammonia-water mixtures with applications. PhD dissertation. University of Michigan; 1988.
[34] Stecco SS, Desideri U. A thermodynamic analysis of the Kalina cycles: comparisons, problems and perspectives. ASME paper 89-GT-149; 1989.
[35] Smolen TM, Manley DB, Poling BE. Vapor–liquid equilibrium data for the NH_3–H_2O system and its description with a modified cubic equation of state. Journal of Chemical and Engineering Data 1991;36(2):202–8.
[36] Moshfeghian M, Shariat A, Maddox RN. Prediction of refrigerant thermodynamic properties by equations of state: vapour liquid equilibrium behaviour of binary mixtures. Fluid Phase Equilibiria 1992;80:33–44.
[37] Ziegler B, C.h. Trepp. Equation of state for ammonia–water mixtures. International Journal of Refrigeration 1984;7(2):101–6.
[38] Ikegami Y, Nishida T, Uto M, Uehara H. Thermophysical properties of ammonia/water by the BWR equation of state. In: Proceedings of the 13th international symposium on thermophysical properties. Japan; 1992, p. 213–16.
[39] Friend DG, Olson AL, Nowarski A. Standard thermophysical properties of the ammonia-water binary fluid. In: Proceedings of the 12th international conference on the properties of water and steam, Orlando, Florida; 1994.
[40] Patek J, Klomfar J. Simple functions for fast calculations of selected thermodynamic properties of the ammonia–water system. International Journal of Refrigeration 1995;18(4):228–34.
[41] Tillner-Roth R, Friend DG. A Helmholtz free-energy formulation of the thermodynamic properties of the mixture water+ammonia. Journal of Physical and Chemical Reference Data 1998;27(1):63–96.
[42] Xu F, Goswami DY. Thermodynamic properties of ammonia–water mixtures for power-cycle applications. Energy 1999;24(6):525–36.
[43] Gillespie PC, Wilding WV, Wilson GM. Vapour–liquid equilibrium measurements on the ammonia–water system from 313 K to 589 K. AIChE Symposium Series 1987;83:97.
[44] Thorin E, Dejfors C, Svedberg G. Thermodynamic properties of ammonia–water mixtures for power cycles. International Journal of Thermophysics 1998;19(2):501–10.
[45] Nowarski A, Friend DG. Application of the extended corresponding states method to the calculation of the ammonia–water mixture thermodynamic surface. International Journal of Thermophysics 1998;19(4):1133–42.
[46] Thorin E. Thermophysical properties of ammonia-water mixtures for prediction of heat transfer areas in power cycles. International Journal of Thermophysics 2001;22(1):201–14.
[47] Mejbri Kh, Bellagi A. Modelling of the thermodynamic properties of the water–ammonia mixture by three different approaches. International Journal of Refrigeration 2006;29(2):211–8.
[48] Polikhronidi NG, Abdulagatov IM, Batyrova RG, Stepanov GV. PVT measurements of water–ammonia refrigerant mixture in the critical and supercritical regions. International Journal of Refrigeration 2009;32(8): 1897–913.
[49] Libotean S, Salavera D, Valles M, Esteve X, Coronas A. Vapour–liquid equilibrium of ammonia+lithium nitrate+water and ammonia+lithium nitrate solution from (293.15 to 353.15) K. Journal of Chemical Engineering Data 2007;52(3):1050–5.
[50] Chaudhari SK, Salavera D, Coronas A. Densities, viscosities, heat capacities, and vapour–liquid equilibria of ammonia+sodium thiocyanate solutions at several temperatures. Journal of Chemical Engineering Data 2011;56(6): 2861–9.
[51] Libotean S, Martin A, Salavera D, Valles M, Esteve X, Coronas A. Densities, viscosities, and heat capacities of ammonia+lithium nitrate and ammonia+lithium nitrate+water solutions between (293.15 and 353.15) K. Journal of Chemical Engineering Data 2008;53(10):2383–8.
[52] Aggarwal MK, Agarwal RS. Thermodynamic properties of lithium nitrate–ammonia mixtures. International Journal of Energy Research 1986;10(1): 59–68.
[53] Infante Ferreira CA. Thermodynamic and physical property data equations for ammonia–lithium nitrate and ammonia–sodium thiocyanate solutions. Solar Energy 1984;32(2):231–6.
[54] Al-Sulaiman FA, Hamdullahpur F, Dincer I. Performance assessment of a novel system using parabolic trough solar collectors for combined cooling, heating, and power production. Renewable Energy 2012;48:161–72.
[55] Schicktanz MD, Wapler J, Henning HM. Primary energy and economic analysis of combined heating, cooling and power systems. Energy 2011;36(1):575–85.
[56] Habibzadeh A, Rashidi MM, Galanis N. Analysis of a combined power and ejector–refrigeration cycle using low temperature heat. Energy Conversion and Management 2013;65 (January):381–91. Global conference on renewable energy and energy efficiency for desert regions 2011 "GCREEDER 2011".
[57] Wang J, Zhao P, Niu X, Dai Y. Parametric analysis of a new combined cooling, heating and power system with transcritical CO_2 driven by solar energy. Applied Energy 2012;94:58–64.
[58] Goswami DY. Solar thermal power—status and future directions. In: Proceedings of the 2nd ISHMT-ASME heat and mass transfer conference, S. Murthy and Y. Jaluria, editors. Tata McGraw Hill, New Delhi; 1995, p. 57–60.
[59] Goswami DY. Solar thermal power technology: present status and ideas for the future. Energy Sources 1998;20(2):137–45.
[60] Goswami DY, Xu F. Analysis of a new thermodynamic cycle for combined power and cooling using low and mid temperature solar collectors. Journal of Solar Energy Engineering 1999;121(2):91–7.
[61] Lu S, Goswami DY. Optimization of a novel combined power/refrigeration thermodynamic cycle. Journal of Solar Energy Engineering 2003;125:212–7.
[62] Lu S, Goswami DY. Theoretical analysis of ammonia-based combined power/refrigeration cycle at low refrigeration temperatures. In: Proceedings of solar sunrise on the reliable energy economy. Reno, Nevada; 2002.
[63] Martin C, Goswami DY. Effectiveness of cooling production with a combined power and cooling thermodynamic cycle. Applied Thermal Engineering 2006;26(5–6):576–82.
[64] Sadrameli SM, Goswami DY. Optimum operating conditions for a combined power and cooling thermodynamic cycle. Applied Energy 2007;84(3):254–65.
[65] Aspen Plus, Version 12.1. Ten Canal Park, Cambridge (MA) 02141: Aspen Technology, Inc; 2004.
[66] Martin C. Study of cooling production with a combined power and cooling thermodynamic cycle. Ph.D thesis. Mechanical and Aerospace Engineering Department, University of Florida, USA; 2004.
[67] Demirkaya G, Padilla RV, Goswami DY, Stefanakos E, Rahman MM. Analysis of a combined power and cooling cycle for low-grade heat sources. International Journal of Energy Research 2011;35(13):1145–57.
[68] Chemcad. Version 6.1.2: Process flow sheet simulator. Chemstations Inc.: Houston; 2008.

[69] Xu F, Goswami DY, Bhagwat SS. A combined power/cooling cycle. Energy 2000;25(3):233–46.
[70] Pouraghaie M, Atashkari K, Besarati SM, Narimen-zadeh N. Thermodynamic performance optimization of a combined power/cooling cycle. Energy Conversion and Management 2010;51(1):204–11.
[71] Vidal A, Best R, Rivero R, Cervantes J. Analysis of a combined power and refrigeration cycle by the exergy method. Energy 2006;31(15):3401–14.
[72] Hasan AA, Goswami DY, Vijayaraghavan S. First and second law analysis of a new power and refrigeration thermodynamic cycle using a solar heat source. Solar Energy 2002;73(5):385–93.
[73] Vijayaraghavan S, Goswami DY. A combined power and cooling cycle modified to improve resource utilization efficiency using a distillation stage. Energy 2006;31(8–9):1177–96.
[74] Vijayaraghavan S. Thermodynamic studies on alternate binary working fluid combinations and configurations for a combined power and cooling cycle. PhD thesis. Mechanical and Aerospace Engineering Department, University of Florida, USA; 2003.
[75] Edgar TF, Himmelblau DM, Lasdon LS. Optimisation of chemical processes. New York: MaGraw-Hill; 2001.
[76] Zare V, Mahmoudi SMS, Yari M. Ammonia–water cogeneration cycle for utilizing waste heat from the GT-MHR plant. Applied Thermal Engineering 2012;48(15):176–85.
[77] Zare V, Mahmoudi SMS, Yari M, Amidpour M. Thermoeconomic analysis and optimization of an ammonia–water power/cooling cogeneration cycle. Energy 2012;47(1):271–83.
[78] Demirkaya G, Besarati S, Padilla RV, Archibold AR, Goswami DY, Rahman MM, et al. Multi-objective optimization of a combined power and cooling cycle for low-grade and midgrade heat sources. Journal of Energy Resources Technology—Transactions of the ASME 2012;134(3) [Art. no. 32002].
[79] Padilla RV, Archibold AR, Demirkaya G, Besarati S, Goswami DY, Rahman MM, et al. Performance analysis of a Rankine cycle integrated with the Goswami combined power and cooling cycle. Journal of Energy Resources Technology, Transactions of ASME 2012;134:3 [Art. no. 32001].
[80] Erickson DC, Anand G, Kyung I. Heat activated dual function absorption cycle. ASHRAE Transactions 2004;110(1):515–24.
[81] Zhang N, Cai R, Lior N. A novel ammonia–water cycle for power and refrigeration cogeneration. In: Proceedings of the ASME advanced energy systems division; 2004. p. 183–96.
[82] Wang J, Dai Y, Gao L. Parametric analysis and optimization for a combined power and refrigeration cycle. Applied Energy 2008;85(11):1071–85.
[83] Liu M, Zhang N. Proposal and analysis of a novel ammonia–water cycle for power and refrigeration cogeneration. Energy 2007;32(6):961–70.
[84] Zheng D, Chen B, Qi Y, Jin H. Thermodynamic analysis of a novel absorption power/cooling combined-cycle. Applied Energy 2006;83(4):311–23.
[85] Zhang N, Lior N. Methodology for thermal design of novel combined refrigeration/power binary fluid systems. International Journal of Refrigeration 2007;30(6):1072–85.
[86] Wang J, Dai Y, Zhang T, Ma S. Parametric analysis for a new combined power and ejector-absorption refrigeration cycle. Energy 2009;34(10):1587–93.
[87] Kiani B, Akisawa A, Kashiwagi T. Thermodynamic analysis of load-leveling hyper energy converting and utilization system. Energy 2008;33(3):400–9.
[88] Zhang N, Lior N. Development of a novel combined absorption cycle for power generation and refrigeration. Journal of Energy Resources Technology 2007;129(3):254–65.
[89] Jawahar CP, Saravanan R. Generator absorber heat exchange based absorption cycle—a review. Renewable and Sustainable Energy Reviews 2010;14(8):2372–82.
[90] Mehr AS, Yari M, Mahmoudi SMS, Soroureddin A. A comparative study on the GAX based absorption refrigeration systems: SGAX, GAXH and GAX-E. Applied Thermal Engineering 2012;44:29–38.
[91] Jawahar CP, Saravanan R, Bruno JC, Coronas A. Simulation studies on gax based kalina cycle for both power and cooling applications. Applied Thermal Engineering 2011. http://dx.doi.org/10.1016/j.applthermaleng.2011.11.004.
[92] REFPROP. Version 9.0: Reference fluid thermodynamic and transport properties database. National Institute of Standards and Technology (NIST), Gaithersburg, USA; 2010. 〈http://www.nist.gov/srd/nist23.cfm〉.
[93] Tamm G, Goswami DY, Lu S, Hasan AA. Theoretical and experimental investigation of an ammonia–water power and refrigeration thermodynamic cycle. Solar Energy 2004;76(1–3):217–28.
[94] Tamm G, Goswami DY. Novel combined power and cooling thermodynamic cycle for low temperature heat sources, Part II: Experimental investigation. Journal of solar energy engineering 2003;125(2):223–9.
[95] Tamm GO. Experimental investigation of an ammonia-based combined power and cooling cycle. Ph.D thesis. Mechanical and Aerospace Engineering Department, University of Florida, USA; 2003.
[96] Goel N. Theoretical and experimental analysis of absorption–condensation in a combined power and cooling cycle. Ph.D thesis. Mechanical and Aerospace Engineering Department, University of Florida, USA; 2005.
[97] Demirkaya G. Theoretical and experimental analysis of power and cooling cogeneration utilizing low temperature heat sources. Ph.D thesis. Mechanical Engineering Department, University of South Florida, USA; 2011.
[98] Bruno JC, Letelier E, Romera S, López J, Coronas A. Modelling and optimisation of solar organic Rankine cycle engines for reverse osmosis desalination. Applied Thermal Engineering 2008;28(17–18):2212–26.
[99] Clemente S, Micheli D, Reini M, Taccani R. Energy efficiency analysis of organic rankine cycles with scroll expanders for cogenerative applications. Applied Energy 2012;97 (September): 792–01.
[100] Quoilin S, Orosz M, Hemond H, Lemort V. Performance and design optimization of a low-cost solar organic Rankine cycle for remote power generation. Solar Energy 2011;85(5):955–66.
[101] Bracco R, Clemente S, Micheli D, Reini M. Experimental tests and modelization of a domestic-scale organic rankine cycle. In: Proceedings of ECOS 2012—The 25th international conference on efficiency, cost, optimization, simulation and environmental impact of energy systems, July 26–29. Perugia, Italy; 2012.